(2)

NAVAL POSTGRADUATE SCHOOL
Monterey, California

THESIS

DOSE ANALYSIS OF THE MODEL 112A PULSERAD PULSED X-RAY GENERATOR BY ITS/CYLTRAN

by

Jong Ryul, Kim

December 1989

Thesis Advisor Xavier K. Maruyama

Unclassified

security classification of this page

REPORT DOCUMENTATION PAGE

1a Report Security Classification: Unclassified	1b Restrictive Markings
2a Security Classification Authority	3 Distribution Availability of Report: Approved for public release; distribution is unlimited.
2b Declassification Downgrading Schedule	
4 Performing Organization Report Number(s)	5 Monitoring Organization Report Number(s)
6a Name of Performing Organization: Naval Postgraduate School; 6b Office Symbol (if applicable): 33	7a Name of Monitoring Organization: Naval Postgraduate School
6c Address (city, state, and ZIP code): Monterey, CA 93943-5000	7b Address (city, state, and ZIP code): Monterey, CA 93943-5000
8a Name of Funding Sponsoring Organization; 8b Office Symbol (if applicable)	9 Procurement Instrument Identification Number
8c Address (city, state, and ZIP code)	10 Source of Funding Numbers: Program Element No; Project No; Task No; Work Unit Accession No

11 Title (Include security classification): DOSE ANALYSIS OF THE MODEL 112A PULSERAD PULSED X-RAY GENERATOR BY ITS CYLTRAN

12 Personal Author(s): Jong Ryul. Kim

13a Type of Report	13b Time Covered From To	14 Date of Report (year, month, day)	15 Page Count
Master's Thesis		December 1989	81

16 Supplementary Notation: The views expressed in this thesis are those of the author and do not reflect the official policy or position of the Department of Defense or the U.S. Government.

17 Cosati Codes			18 Subject Terms (continue on reverse if necessary and identify by block number)
Field	Group	Subgroup	Flash X-Ray, ITS CYLTRAN, Monte Carlo

19 Abstract (continue on reverse if necessary and identify by block number)

The radiation output from the NPS Pulserad 112A X-ray Generator has been calculated using the ITS code CYLTRAN. The results of this numerical simulation have been compared to the experimental measurements taken previously. These calculations show that the overall photon energy spectrum is independent of the electron source beam parameters such as beam radius and angular distribution. A previously unexplained measured dip in the radiation dose at the beam center line can be explained with an angular divergence of the electron beam from the cathode. The simulation is successful in explaining the pattern of the dose distribution, but the calculation is in general much smaller than the measured values. This inability to reproduce the magnitude of the dose pattern points out the need to measure the radiation dose each time the Pulserad 112A is used. Some suggestions for explaining this discrepancy are included.

20 Distribution Availability of Abstract	21 Abstract Security Classification	
☒ unclassified unlimited ☐ same as report ☐ DTIC users	Unclassified	
22a Name of Responsible Individual: Xavier K. Maruyama	22b Telephone (include Area code): (408) 646-2431	22c Office Symbol: 54Ss

DD FORM 1473,84 MAR 83 APR edition may be used until exhausted
All other editions are obsolete

security classification of this page

Unclassified

Approved for public release; distribution is unlimited.

Dose Analysis of the Model 112A Pulserad
Pulsed X-Ray Generator by ITS/CYLTRAN

by

Jong Ryul, Kim
Major, Republic of Korea Army
B.S., Republic of Korea Military Academy, 1980

Submitted in partial fulfillment of the
requirements for the degree of

MASTER OF SCIENCE IN PHYSICS

from the

NAVAL POSTGRADUATE SCHOOL
December 1989

Author: _____
Jong Ryul, Kim

Approved by: _____
Xavier K. Maruyama, Thesis Advisor

_____
J.R. Neighbour, Second Reader

_____
Karlheinz E. Whoeler, Chairman,
Department of Physics

ABSTRACT

The radiation output from the NPS Pulserad 112A X–ray Generator has been calculated using the ITS code CYLTRAN. The results of this numerical simulation have been compared to the experimental measurements taken previously. These calculations show that the overall photon energy spectrum is independent of the electron source beam parameters such as beam radius and angular distribution. A previously unexplained measured dip in the radiation dose at the beam center line can be explained with an angular divergence of the electron beam from the cathode. The simulation is successful in explaining the pattern of the dose distribution, but the calculation is in general much smaller than the measured values. This inability to reproduce the magnitude of the dose pattern points out the need to measure the radiation dose each time the Pulserad 112A is used. Some suggestions for explaining this discrepancy are included.

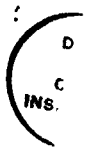

TABLE OF CONTENTS

ACKNOWLEDGEMENTS

I wish to express my sincere thanks and appreciation to all of the people without whose help this thesis could have been much more difficult if not impossible.

A special thank you to my thesis advisor, Dr. Xavier K. Maruyama, who not only took on a challenge by accepting me as a thesis student, but who was also extremely patient as I acquired the skills necessary to complete this thesis.

I would also like to thank Rick Philips for his time and effort spent to modify ITS/CYLTRAN codes and ensure the codes were accurately executing

Finally many thanks to my wife Jung–Sook and my daugther Sah–Rang, who never complained about days that we have spent in Monterey, California.

I. INTRODUCTION

The Model 112A Pulserad Pulsed X–Ray Generator installed at the Naval Postgraduate School was built by the Physics International Company. Installation in the new Flash X–ray Facility was completed in August of 1988. This system is a high power x–ray source. The radiation is produced in a three step process. The twelve stage Marx Generator is charged via an external power supply to the desired voltage. The Blumlein Pulse Forming line is then resonance charged from the Marx Generator. When fully charged the Blumlein discharges rapidly into the electron accelerator tube creating a large potential difference across the diode gap. The cathode consists of a stainless steel rod which readily emits electrons when the high voltage is applied. The electrons are accelerated across the anode–cathode spacing until they impact a tantalum target. The resulting bremsstrahlung process produces radiation.

A. PREVIOUS EXPERIMENT ON RADIATION OUTPUT

The use of the Model 112A Pulserad Pulsed X–Ray Generator in radiation effects study requires some knowledge of the characteristics of the output radiation. The experiment to measure the magnitude of the radiation field was performed by R. B. Pietruszka [Ref. 1] using the dosimetry system which consists of Thermoluminescent Dosimeter (TLD) and associated TLD readers. The primary TLD's were CaF_2:Mn chip dosimeters and the TLD readers were Victoreen Model 2800 and Model 2800M. This was the initial radiation mapping of the flash x–ray machine as a function of the system parameters. Since the Marx charge voltage is

the primary variable controlled by the operator, this experiment was to measure exposure at various Marx charge voltages.

When the radiation field was measured at the faceplate, one of the characteristics of the radiation pattern is that the maximum exposure did not occur at the geometric center of the anode assembly. The average radius of the relative maxima was 1.3 ± 0.6 cm from the center. A typical pattern is shown in Figure 1.

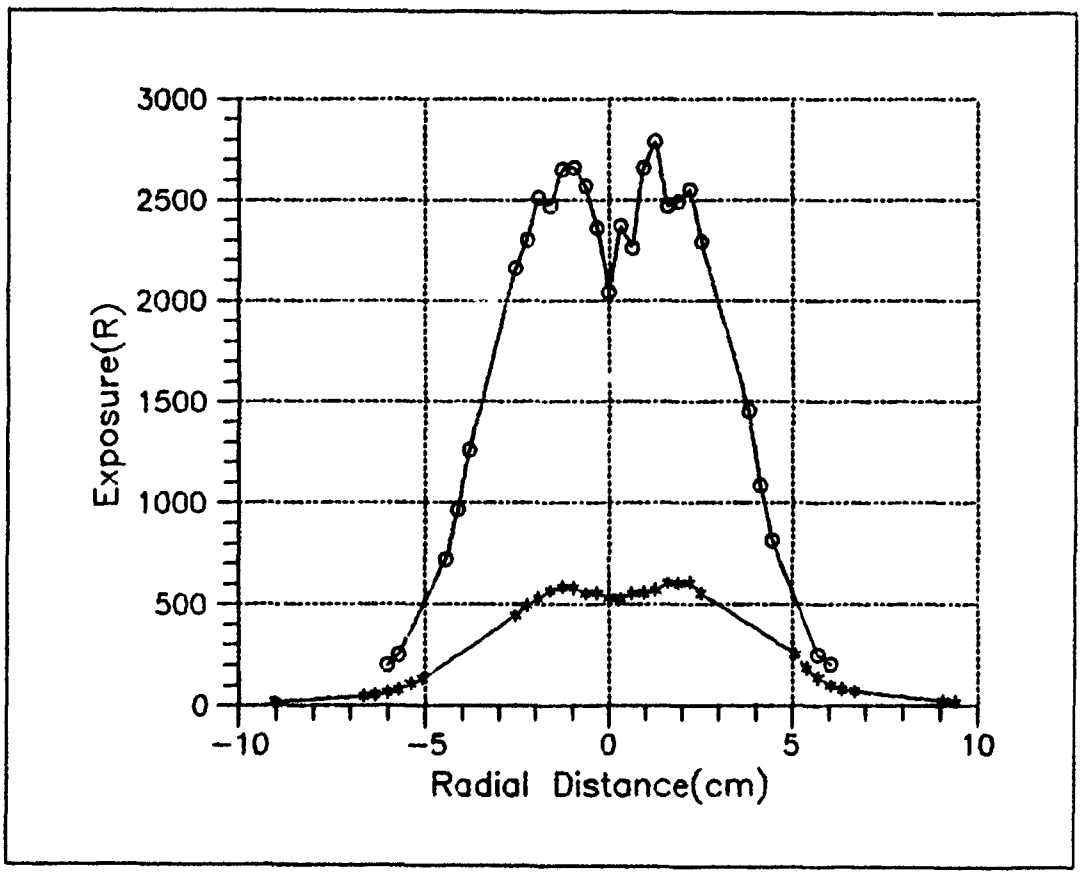

Figure 1. Typical Pulsrad 112A Exposure Pattern at the Anode Face Plate. (Circles are at 100 kV Marx Charge, Stars at 75 kV Marx Charge)

Variations in the exposures recorded were also observed between shots made at the same Marx charge voltage (see Appendix F). This variations are summarized in Table I for Marx charge voltage of 75 kV and 100 kV. Corresponding peak electron energy measured was 1.34 MeV for 75 kV and 1.66 MeV for 100 kV

TABLE I : VARIATION OF EXPOSURE MEASURED AT GEOMETRIC CENTER OF ANODE ASSEMBLY [Ref. 1]

Marx Voltage	75 KV	100 KV
Peak Diode Voltage	1.34 MV	1.66 MV
Minimum Peak Exposure	432 R	2040 R
Maximum Peak Exposure	895 R	3090 R
Mean Exposure	600 ± 150 R	2600 ± 340 R

B. ITS/CYLTRAN

ITS (Integrated TIGER series of coupled electron/photon Monte Carlo Transport Codes) is the most widely used computer code to predict radiation output generated from flash x–ray sources, as well as subsequent photon/electron transport and energy deposition in materials located downstream of the source. The release version 2.1 (February 1987) has been installed in the IBM main frame at Naval Postgraduate School and the release version 2.0 (July 1986) has also been installed on the micro VAX 3200 workstation in nuclear physics laboratory.

The CYLTRAN code is a member code of the ITS system that is specially designed for applications having approximately azimuthal symmetry. CYLTRAN simulates the transport of particle trajectories through a three–dimensional multimaterial cylinder. For this thesis, only the CYLTRAN code was required. CYLTRAN, like all members of ITS system, contains the essential physics for generating and transporting the complete electron/photon cascade until these particles either are absorbed, escape from the system, or have their energies reduced below some user defined cutoffs. For more details of ITS/CYLTRAN see Appendix E.

C. PURPOSE

In the present paper, the intensity of radiation field of the Model 112A Pulserad Pulsed X–Ray Generator is computed using the CYLTRAN code. The simulated outputs at the anode faceplate of the flash x–ray machine are compared with the experimental results in chapter III. The characteristic radiation pattern "dip" at the anode faceplate is utilized to investigate the electron source beam parameters such as effective cathode radius and angle of electron main flow. The radiation dosage in TLD's at the various axial distance is also calculated using CYLTRAN and compared with the design dose output.

II. CALCULATION OF ABSORBED DOSE FROM MEASURED EXPOSURE

A. PROCEDURES

Since the CYLTRAN output is in terms of 'absorbed dose', the measured exposures should also be expressed as absorbed dose in order to compare each other. The absorbed dose in a medium can be determined from the measured exposures by following three equations (1) to (3). We have already the values of average exposure at 75 kV Marx charge and 100 kV Marx charge. In order to calculate the absorbed dose in a medium CaF_2:Mn, the following procedures were taken.

(a) Calculate the absorbed dose in air (D_{air}) using equation (1).

(b) Calculate the average photon energy absorption coefficients for air and CaF_2:Mn. using equation (3)

(c) Calculate the absorbed dose in CaF_2:Mn using equation (2).

Under conditions of CPE, the absorbed dose is directly determined by the measurement of collision kerma, K_c, and exposure, X.[Ref. 5]

(1) $$D_{air} = (K_c)_{air} = 0.876\ X \quad (\text{for CPE})$$

where $(K_c)_{air}$ and D_{air} are in rads, and X in roentgens.

The formal definition of CPE is "a condition that exists in a material under irradiation if the energies, number, and direction of charged particles induced by the radiation are constant throughout the volume of interest, Therefore, within such a

volume, the sum of energies of all charged particles entering it is equal to the corresponding sum for all particles leaving it."[Ref. 12]. Moreover, if the same photon energy fluence Ψ' is present in media A and B having two different average energy absorption coefficients $(\mu_{en}/\rho)_a$ and $(\mu_{en}/\rho)_b$, the ratio of the absorbed doses under CPE conditions in the two media will be given by

$$(2) \qquad \frac{D_a}{D_b} = \frac{(K_c)_a}{(K_c)_b} = \frac{\overline{(\mu_{en}/\rho)_a}}{\overline{(\mu_{en}/\rho)_b}} \qquad \text{(for CPE)}$$

where

$\overline{(\mu_{en}/\rho)_a}$ and $\overline{(\mu_{en}/\rho)_b}$; average energy absorption coefficients

$$(3) \qquad \overline{\left(\frac{\mu_{en}}{\rho}\right)} = \frac{\int_E \Psi'(E) \left(\frac{\mu_{en}}{\rho}\right) dE}{\int_E \Psi'(E)\, dE}$$

Appendix D further elaborates on the terminology and definition used in these procedures.

B. CALCULATION

Since the values of exposure were measured the procedure (a) is simple to obtain. In order to calculate the average photon energy absorption coefficients, however the spectrum of photon energy fluence $\Psi'(E)$ is required. This distribution of photon energy can be obtained by running ITS According to ICRU(International Commission in the Radiation units and Measurements), the particle fluence of monoenergetic photons is defined as the differential quotient of the number of particles dN that cross a sphere of cross–sectional area da:

$$\Psi = dN/da$$

This definition is not practical from a calculational point of view as it is based on the geometrical properties of a sphere. However, by multiplying both dN and da by the mean cord length $\bar{l} = 4V/A$, a more practical definition can be obtained. As $\bar{l}dN$ is equal to the mean pathlength $\overline{ds}$ in the sphere, and $\bar{l}da$ is the volume dV of the sphere, the above equation becomes

$$\Psi = \overline{ds} / dV,$$

which is independent of the shape of the volume, and can be interpreted as the "track length per unit volume". The distribution in photon energy fluence, Ψ', can be calculated by ITS/CYLTRAN in terms of the "photon track length per unit volume" in a specific region of the test medium.

There is another way of getting the incident photon energy fluence by ITS. The number of incident photons at a defined energy dE per unit area at (r,θ), $dN(E,\theta)$, can be calculated.(see Figure 2. Target Geometry). The incident photon fluence Ψ' on the forward hemisphere of the photon target located at r is then

$$\Psi'(E,\theta) = E \cdot \frac{dN(E,\theta)}{dE}$$

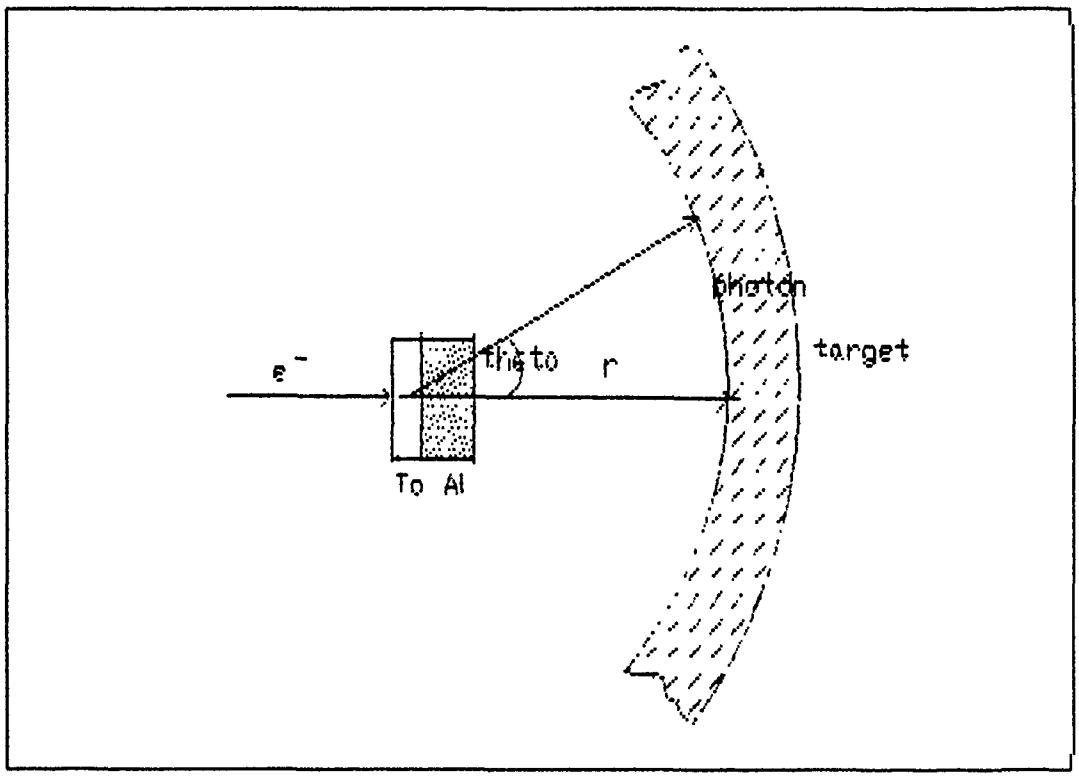

Figure 2. Photon Target Geometry

Let us take a spectrum of the photon energy transmitted at the anode face plate which is calculated by ITS/CYLTRAN. This photon energy spectrum is normalized to one incident electron and shown in the Table IV and Figure 3. Obviously the average photon energy transmitted is less than the maximum energy and it is about 1/5 times of the maximum photon energy. More details of getting the overall photon energy spectrum will be discussed in the next chapter. The average energy absorption coefficients in air and in CaF_2:Mn can be calculated from this photon energy fluence. This photon fluence is presented graphically in Figuree 4. The absorbed dose in a test medium CaF_2:Mn from the measured values of exposure can also obtained using those average energy absorption coefficients.

TABLE II : ENERGY SPECTRUM OF TRANSMITTED PHOTONS CALCULATED FROM CYLTRAN AT MARX CHARGE OF 100 KV AT ANODE FACE PLATE (normalized to one incident electron)

Energy (MeV)	Photons (#/SR–MeV)	Photon Fluence(MeV/Area)
1.66 – 1.40	8.37 E –05	1.26 E –04
1.40 – 1.3	9.37 E –04	1.27 E –03
1.3 – 1.2	1.24 E –03	1.55 E –03
1.2 – 1.1	3.50 E –03	4.03 E –03
1.1 – 1.0	3.68 E –03	3.86 E –03
1.0 – 0.9	5.64 E –03	5.36 E –03
0.9 – 0.8	1.00 E –02	8.50 E –03
0.8 – 0.7	1.16 E –02	8.70 E –03
0.7 – 0.6	1.81 E –02	1.18 E –02
0.6 – 0.5	3.17 E –02	1.74 E –02
0.5 – 0.4	4.34 E –02	1.95 E –02
0.4 – 0.3	7.15 E –02	2.50 E –02
0.3 – 0.2	1.07 E –01	2.68 E –02
0.2 – 0.1	1.11 E –01	1.67 E –02
0.10 – 0.05	1.28 E –01	9.60 E –03
Total	4.51 E –01	1.36 E –01

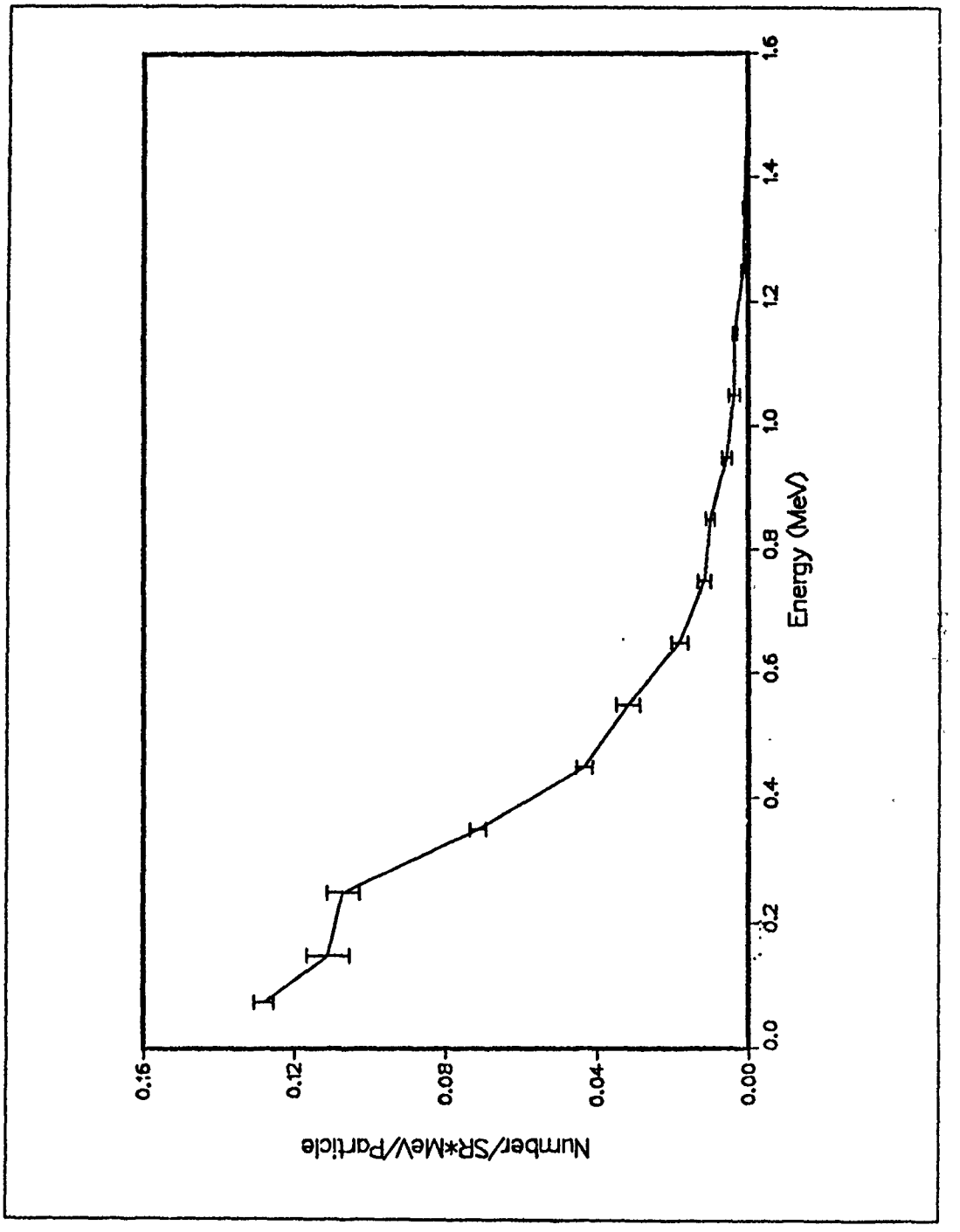

Figure 3. Calculated Photon Energy Spectrum Transmitted through Anode Face Plate at a Marx Charge of 100 kV.(Normalized to One Incident Electron)

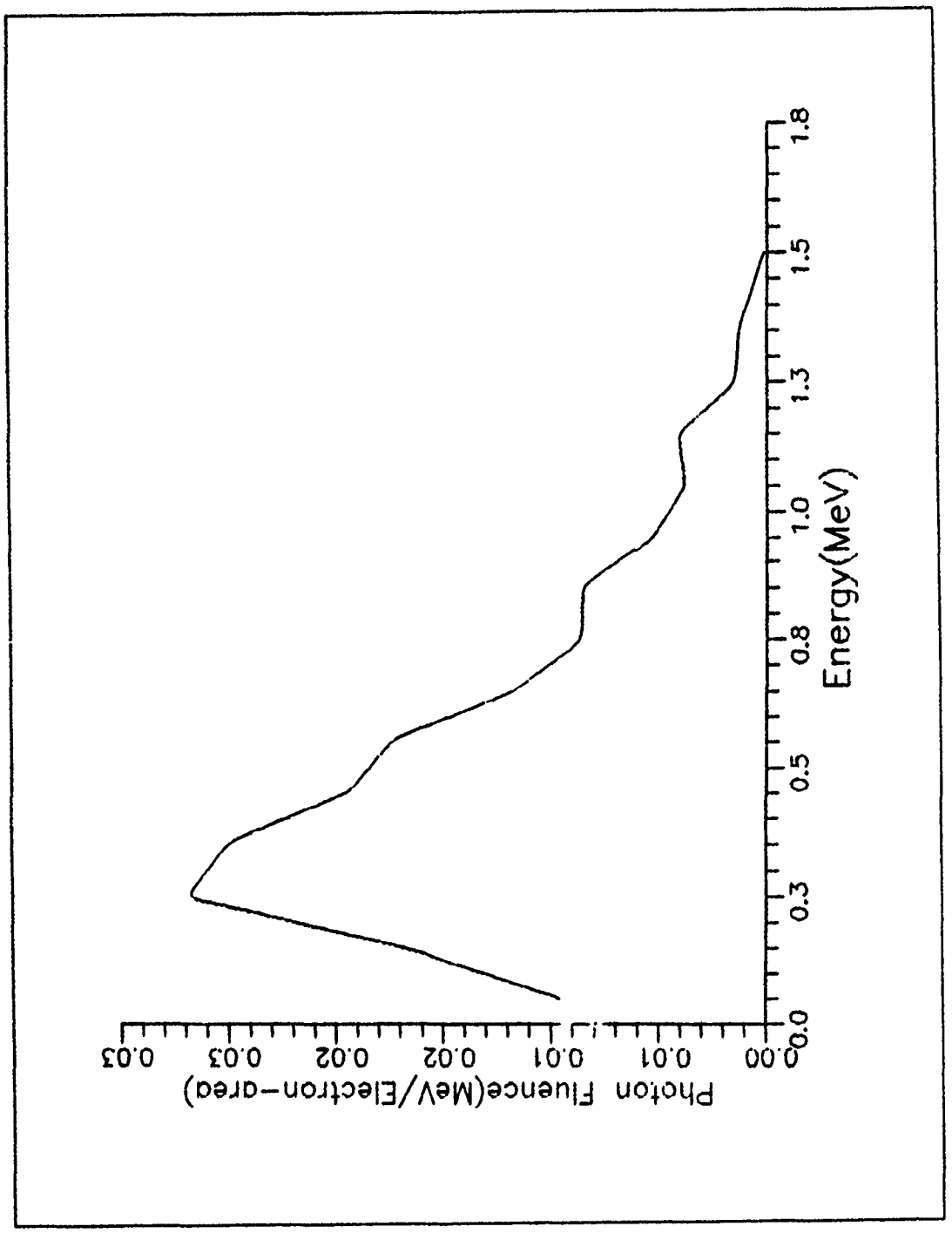

Figure 4. Calculated Photon Fluence at Anode Face Plate at a Marx Charge of 100 kV.(Normalized to One Incident Electron)

The result of calculation of the ratio of the two average energy absorption coefficients using equation (3) is as follows

$$\overline{(\mu_{en}/\rho)}_{CaF_2Mn} \; / \; \overline{(\mu_{en}/\rho)}_{air} \quad = \quad 2.222$$

If the measured exposure is X (roentgen), then the absorbed dose in CaF_2:Mn is (0.876×2.222) × X (rad) for this particular photon energy fluence. The calculation of the average energy absorption is shown in the following Table V. This method of calculating the absorbed dose in the test material from the measured exposures will be applied in the following chapter and those absorbed doses will be compared with the simulation results.

TABLE III : CALCULATION OF RATIO OF THE AVERAGE ENERGY ABSORPTION COEFFICIENTS

Energy	Photons	Photon Fluence	(μ_{en}/ρ) air	(μ_{en}/ρ) CaF_2Mn	$\Psi' \times ((\mu_{en}/\rho)$ air	CaF_2Mn
(MeV)	(#/Sr–MeV)	(MeV/area)	(m^2/kg)		(MeV/kg)	
1.66–1.4	8.37E–5	1.26E–4	0.0254	0.0247	3.20E–6	3.11E–6
1.40–1.3	9.37E–4	1.27E–3	0.0266	0.0262	3.38E–5	3.33E–5
1.3 –1.2	1.24E–3	1.55E–3	0.0269	0.0265	4.17E–5	4.11E–5
1.2 –1.1	3.50E–3	4.03E–3	0.0273	0.0267	1.10E–4	1.08E–4
1.1 –1.0	3.68E–3	3.86E–3	0.0278	0.0270	1.07E–4	1.06E–4
1.0 –0.9	5.64E–3	5.36E–3	0.0285	0.0276	1.53E–4	1.48E–4
0.9 –0.8	1.00E–2	8.50E–3	0.0289	0.0281	2.46E–4	2.39E–4
0.8 –0.7	1.16E–2	8.70E–3	0.0292	0.0285	2.54E–4	2.48E–4
0.7 –0.6	1.81E–2	1.18E–2	0.0295	0.0290	3.48E–4	3.13E–4
0.6 –0.5	3.17E–2	1.74E–2	0.0295	0.0292	5.13E–4	5.08E–4
0.5 –0.4	4.34E–2	1.95E–2	0.0296	0.0295	5.77E–4	5.75E–4
0.4 –0.3	7.15E–2	2.50E–2	0.0290	0.0296	7.25E–4	7.40E–4
0.3 –0.2	1.07E–2	2.68E–3	0.0275	0.0306	7.37E–5	8.20E–5
0.2 –0.1	1.11E–1	1.67E–2	0.0250	0.0397	4.17E–4	6.63E–4
0.1–0.05	1.28E–1	9.60E–3	0.0406	0.436	3.90E–4	4.19E–3
TOTAL		1.36E–1			3.60E–3	8.00E–3

III. RADIATION DOSE ANALYSIS USING ITS/CYLTRAN

The use of the Model 112A pulserad pulsed x–ray generator in radiation experiments requires knowledge of the characteristics of the output radiation. The experiment to measure the exposure at various axial/angular distance was done by Renee B. Pietruszka. Although the measured values have some variations from shot to shot, those measured exposures are the basis of this radiation dosage analysis. In order to compare the measured values with the results obtained by running the ITS, the experimental configurations at 75 kV and 100 kV Marx charge voltage were modeled with ITS/CYLTRAN codes. The dosimetry analysis using ITS/CYLTRAN was divided into three principal parts :

1. Determination of the photon energy spectrum
2. Investigation of electron source beam parameters by comparison between measured radiation pattern and simulation results
3. Determination of the intensity of the radiation at different axial distance.

A. SIMULATION ENTRIES

1. Electron Accelerator Tube

The electron accelerator tube is a field emission diode mounted in a vacuum. The cathode is a cylindrical stainless steel rod which tapers from a shank diameter of 3.2 cm (5/4 inch) to a tip diameter of 1.9 cm (3/4 inch). Either end of the cathode may be used for electron beam generation. The experiments to

measure exposures were made with the 3.2 cm (5/4 inch) end as the electron emission source.

The anode, which acts as the bremsstrahlung target, is made from a sheet of 0.381 mm (0.015 inch) tantalum. The tantalum is protected by a 0.64 cm (1/4 inch) thick aluminum faceplate. The anode–cathode spacing should have been 2.54 cm which is specified in the Pluserad 112A Operations Manual. However, when measured, the anode–cathode spacing was found to be 17.5 mm. The diagram of the electron accelerator tube is depicted in Appendix C.

2. Electron Beam Energy

a. Measured Diode Voltage and Current

The Marx Output Voltage was monitored during the previous experiments using the two voltage monitors. These monitors (PIM –197) are $CuSO_4$ resistors The current across the diode was also monitored with the Model 199 Fluxmeter. It consists of a loop that is mounted in the diode vacuum envelope. The changing magnetic field in the diode vacuum envelope induces a current in the loop. The resulting voltage pulse in the "$\dot{B}$–probe" is output from the monitor. The magnetic field and the current in the diode can then be calculated. Table VI summarizes the results of data taken at Marx charging voltages of 75kV and 100kV.

TABLE IV : MEASURED DIODE VOLTAGE AND CURRENT FOR PULSERAD 112A.[Ref. 1]

Marx Charge (kV)	Diode Voltage (MV)	Diode Current (kA)
75	1.34 ± 0.03	11.0 ± 1
100	1.66 ± 0.03	20.5 ± 1

The following two figures (Fig. 5, Fig. 6) are photographs of typical diode voltage waveforms monitored by the Tektronix 7104 Oscilloscope. The half–width at half–maximum of both pulses is approximately 30 ns. These figures indicate that the electron beam is not monoenergetic. The energy distribution of the electron beam can be figured from these photographs. The photographs of diode current waveforms also were taken during the experiment. They are shown in Figure 7 and Figure 8. The half–width at half–maximum of these current pulses are 20 ns. The total electron flow during the pulse, which is needed for the calculation of absorbed dose in a test medium, can be extracted from these current waveform photographs. Calibration of these monitored pulses including monitor sensitivity and attenuation ratio of voltages in and out was described in Reference 1.

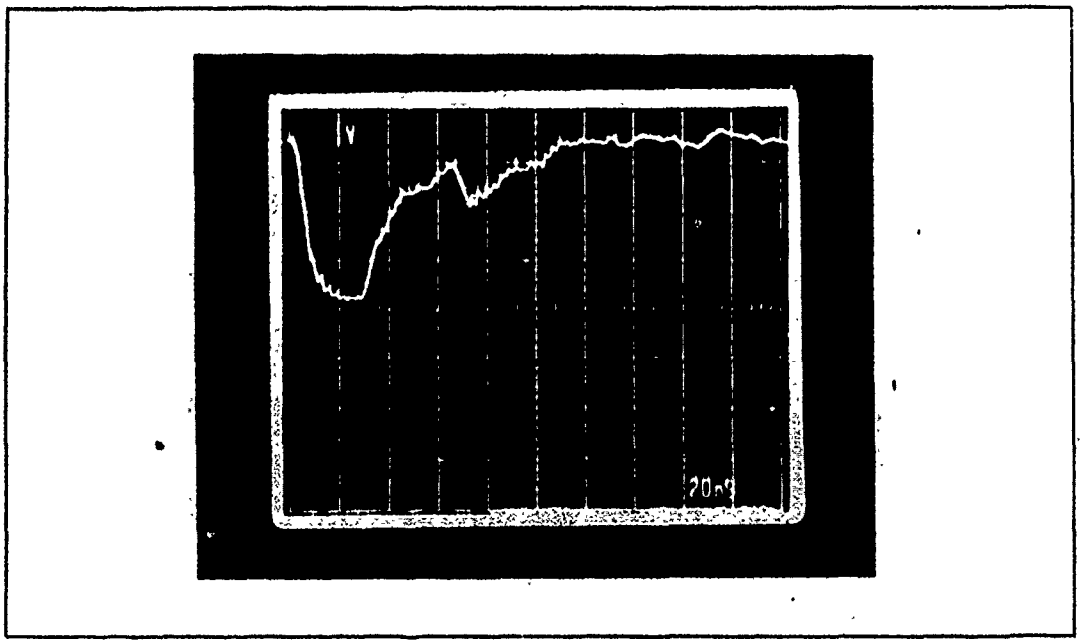

Figure 5. Photograph of Typical Diode Voltage Waveform at Marx Charge 75 kV (horizontal scale 20 ns/cm, peak voltage 1.2 MV).

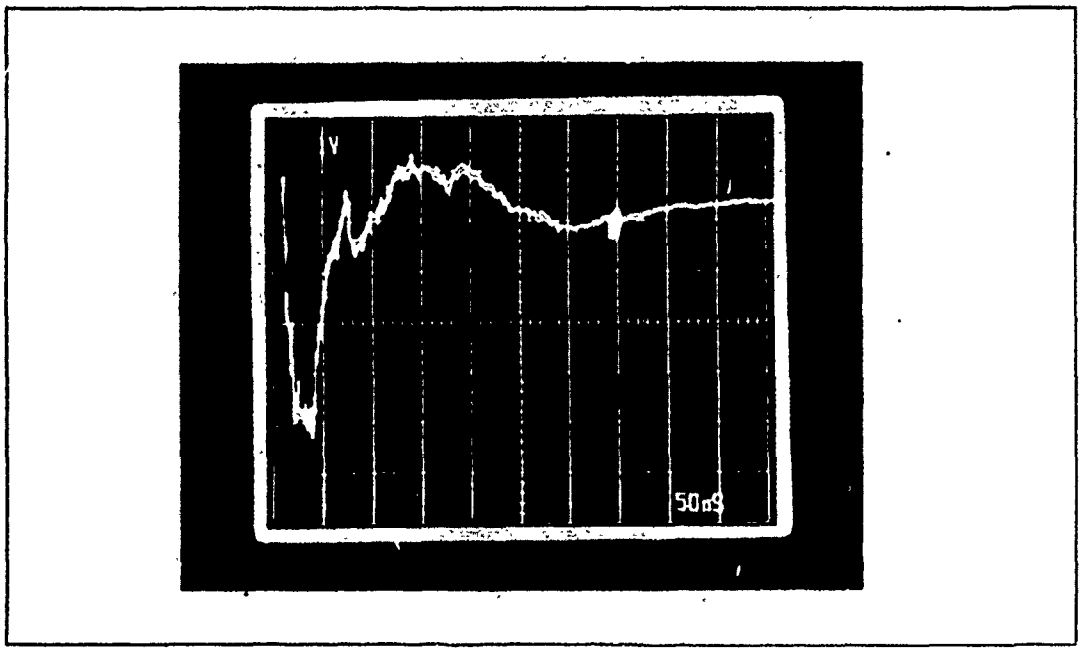

Figure 6. Photograph of Typical Diode Voltage Waveform at Marx Charge 100 kV (horizontal scale 50 ns/cm, peak voltage 1.7 MV)

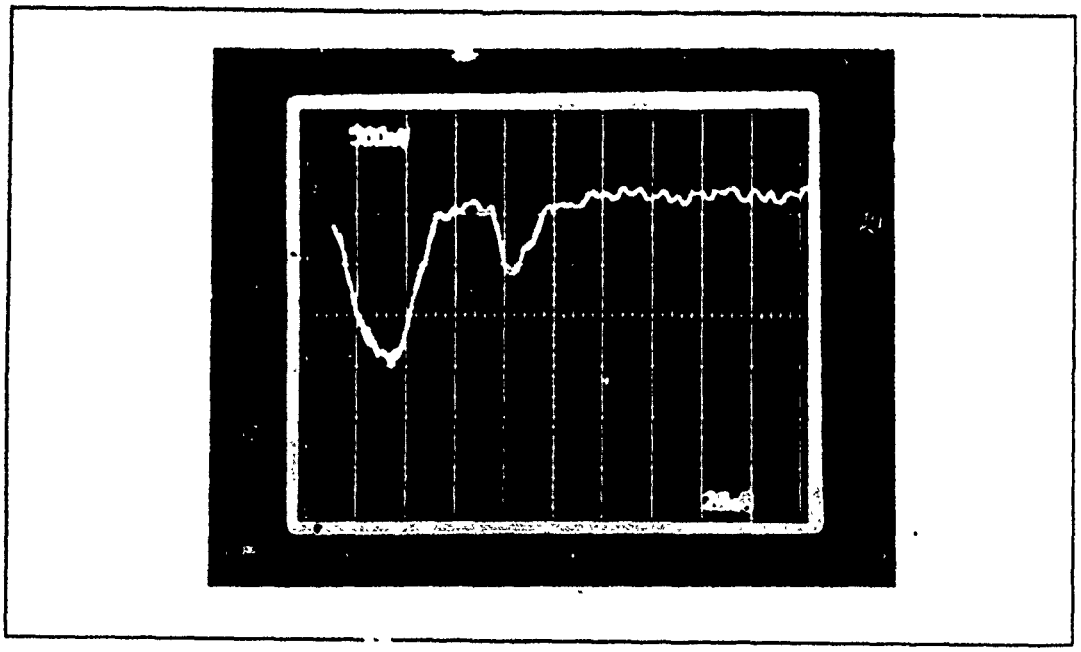

Figure 7. Photograph of Typical Diode Current Waveform at the Marx Charge Voltage 75 kV (horizontal scale 20 ns/cm, peak current 11 kA))

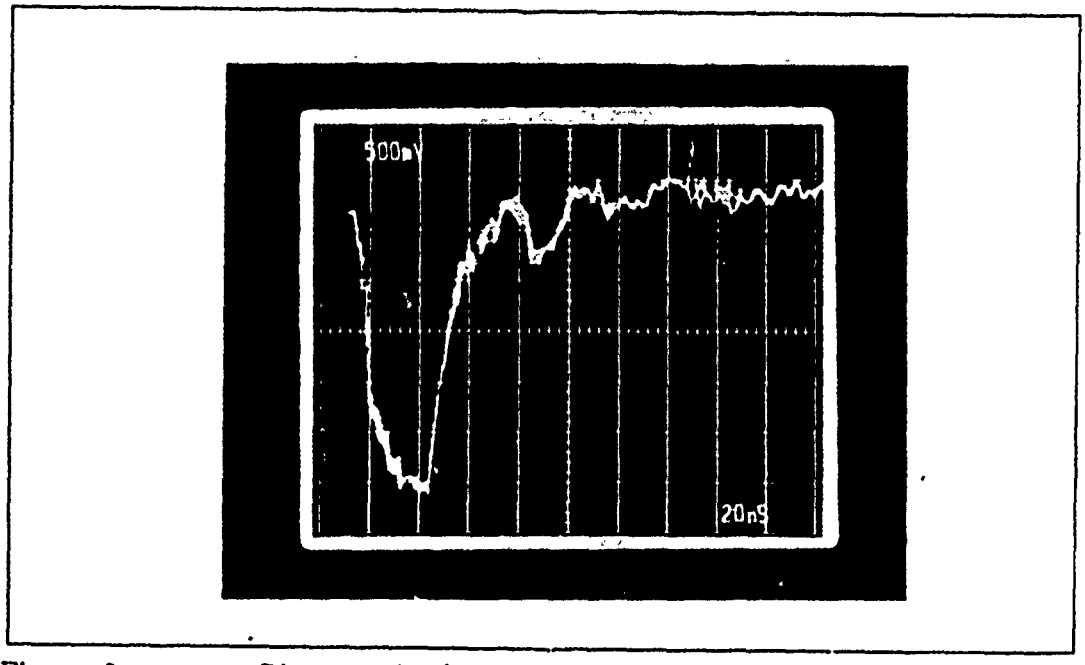

Figure 8. Photograph of Typical Diode Current Waveform at The Marx Charge Voltage 100 kV (horizontal scale 20 ns/cm, peak current 20.9 kA).

b. Theoretical Diode Current and Voltage Outputs

The voltage across the accelerator tube can be calculated by the following way.[Ref. 3]

$$V_t = 2 \times V_2 \times \frac{Z_t}{Z_t + Z_b}$$

$$V_2 = 12 \times 1.2 \times 0.9 \times V_0$$

where

V_t = Accelerator tube Voltage

V_2 = Blumlein Pulse Charge Voltage

V_0 = Marx Charge Voltage

Z_t = Accelerator tube Impedance

Z_b = Blumlein Impedance

The resulting diode current (I_t) can then be computed from Ohm's law:

$$I_t = \frac{V_t}{Z_t}$$

The following table summarizes the theoretical results of calculations for various Marx charging Voltages.

TABLE V : THEORETICAL VOLTAGE AND CURRENT PARAMETERS FOR PULSERAD 112A [Ref. 1]

V_0 (Marx) (kV)	V_b(Blumlein) (MV)	V_t (Tube) (MV)	I_t (Tube) (kA)
75	0.97	1.04	20.90
100	1.30	1.39	27.87

There is a significant difference between the calculated and measured values (see Table VIII). The measured impedance ($Z_t = V_t/I_t$) was found to be 122 ohms at Marx Charge 75 kV and 80 ohms at Marx Charge 100 kV which are different from the specified electron tube impedance value of 50 ohms. This may be caused from the fact that the cathode–anode seperation was smaller. The further investigation of diode spacing is needed. The measured values were used for the input data to analyze the dosage patterns in the following Chapters. The next table campares the theoretical voltage/current with the measured voltage/current.

TABLE VI : COMPARISON BETWEEN THEORETICAL DIODE VOLTAGE/CURRENT AND MEASURED DIODE VOLTAGE/CURRENT

Marx Voltage (kV)	Diode Voltage		Diode Current	
	Measured (MV)	Calculated (MeV)	Measured (kA)	Calculated (kA)
75	1.34±.03	1.04	11.0±1	20.9
100	1.66±.03	1.39	20.5±1	27.9

B. DETERMINATION OF PHOTON ENERGY SPECTRUM

The first step to obtain the radiation output of the Model 112A Pulserad Pulsed X–Ray Generator is to determine the Photon energy spectrum. The Photon energy spectrum was obtained by running ITS. The measured parameters of the electron beam accelerator and its measured beam energy, which are specified in the previous section A, were used as input data. Although the input parameters should be the same as in the Flash X–ray machine, there are several unknown parameters that are necessary for the simulation input.

The first unknown parameter is the radius of the electron source beam. The beam radius may not be the same as the radius of the cathode. In other words the effective cathode radius may be larger than the physical cathode radius. Futher investigation on this point will be done in the next section B. Three sets of the beam radii were entered for the overall photon energy spectrum which is normalized to one incident electron.

The second parameter is the beam propagation angle. Because the dominant electron flow mode may be parallel to the electrostatic field lines of force, the source beam would be truncated at a certain angle with respect to the center direction. The key words "isotropic" and "cosine–law" are used in ITS/CYLTRAN for the source electron angular distribution. The word "isotropic" defines angular distribution of source particles as being isotropic with respect to the reference direction, and the word "cosine–law" defines angular distribution of source electrons as being proportional to the cosine of the specified angle with respect to the reference direction. The distribution is truncated at a given angle in both keywords. The angles 30, 45 and 60 degrees for both "isotropic" and "cosine–law" were entered to

investigate the overall photon energy spectrum. Results for monodirectional flow with all electrons parallel from cathode to anode is also calculated.

The third ambiguous factor is the energy distribution of the electron beam. Photographs of the diode voltage wave form were taken for the duration of the pulse. The measured diode voltage and current are different from the theoretical values. Because the photographs of diode current waveform and diode voltage waveform are available, the measured values of diode voltage were used for the overall photon energy spectrum. From those photographs the energy spectrum of electron source beam is simplified for the simulation input by applying a histogram fit to the typical diode waveform(see Fig. 9).

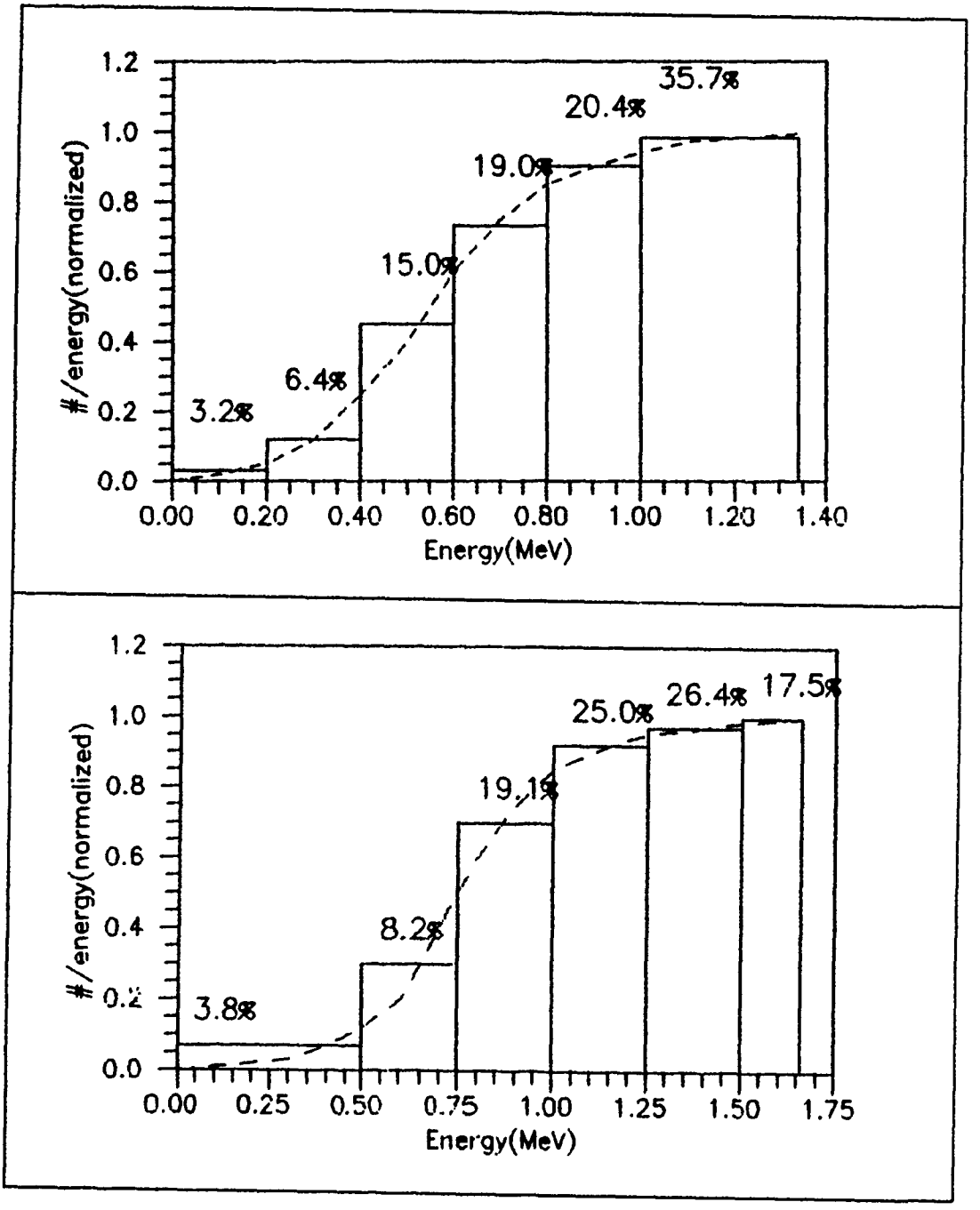

Figure 9. Distribution of the Beam Energy Content for 75 kV Marx Charge(upper) and 100 kV Marx Charge(lower).

1. Input

The radius of the electron source beam, the angle of the electron flow mode, and the beam energy distribution used for determining the overall spectrum of transmitted photon energy were shown in the Table VIIII. The simulation geometry is depicted in Figure 10. The actual input file for running ITS/CYLTRAN is in Appendix A.

TABLE VII : INPUT DATA

beam radius	– 5/8 inch(1.86 cm) – 1 inch(2.54 cm) – 3/2 inch(3.81 cm)
source	electrons
diode space	1.75 cm
anode	TA : 0.0381 cm thick AL : 0.635 cm thick
anode radius	10 cm
beam energy	– monoenergetic beam 1.34 MeV at Marx charge 75 kV 1.66 MeV at Marx charge 100 kV – spectrum type beam see Fig.8
cutoffs	0.05 MeV
angular distribution	– monodirectional(perpendicular to anode) – isotropic 30, 45 and 60 degrees – cosine–law 30, 45 and 60 degrees
histories	35,000

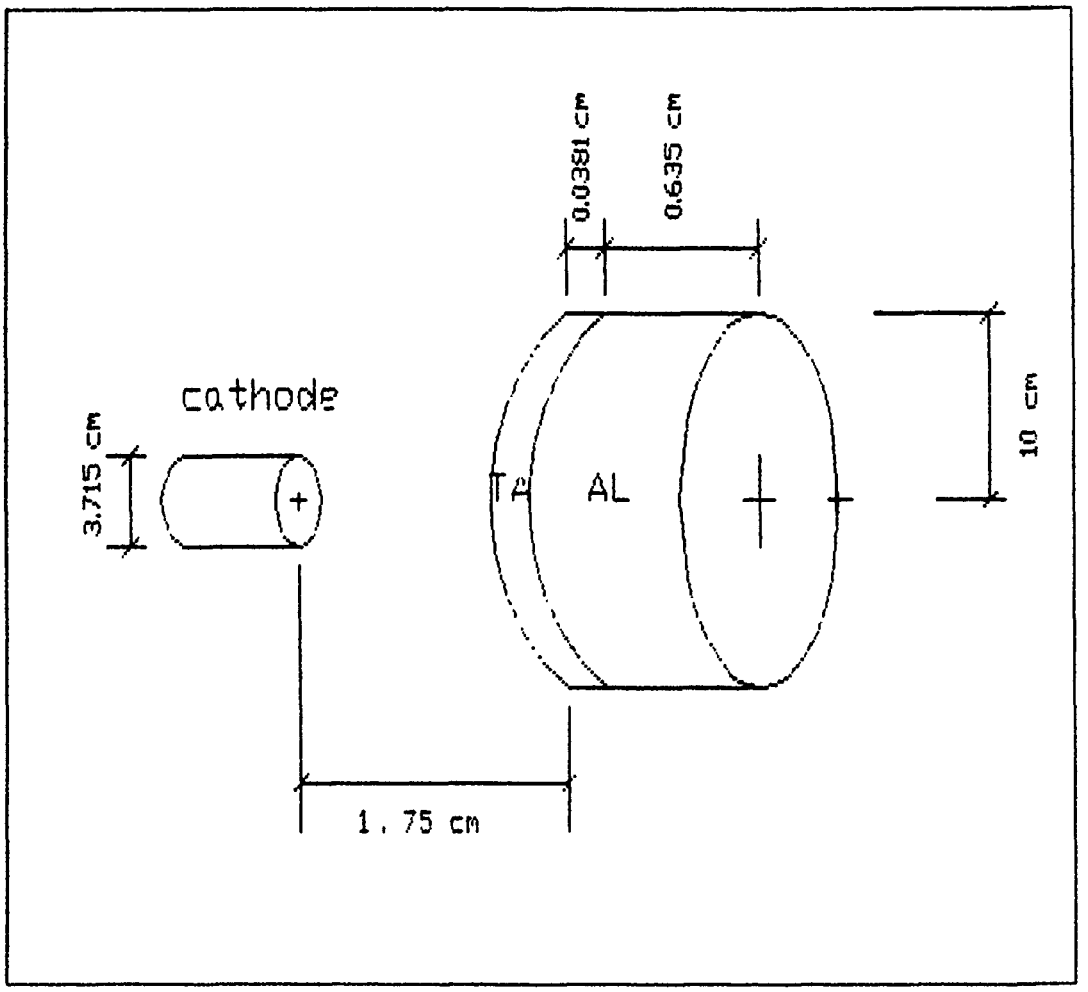

Figure 10. Geometry Configuration entered into CYLTRAN

2. Output

Tne outputs of the transmitted photon energy spectra are normalized to one incident particle. The photon energy spectrum for both the monoenergetic electron source beam and the spectrum type source beam are presented in the Fig 11. and Fig 12. The photon energy spectrum of the spectrum source beam is about twice that of the monoenergetic beam at both 75 kV Marx voltage and 100 kV marx charge. This result is reasonable as the average energy of the spectrum source is much less than that of the monoenergetic beam.

Although the electron source beam is expanding in the vacuum tube with a certain angle with respect to the reference direction, the overall energy spectrum of the transmitted photon remains almost the same. The comparison of the photon energy spectrum for the different angular distribution of electron beam is shown in figures 13, 14 and 15. These figures shows that the overall transmitted photon energy spectrum is independent on the angular distribution of electron source beam.

For three different cathode radii the photon energy spectra also appear to be the same. This phenomenon is presented in Figure 16.

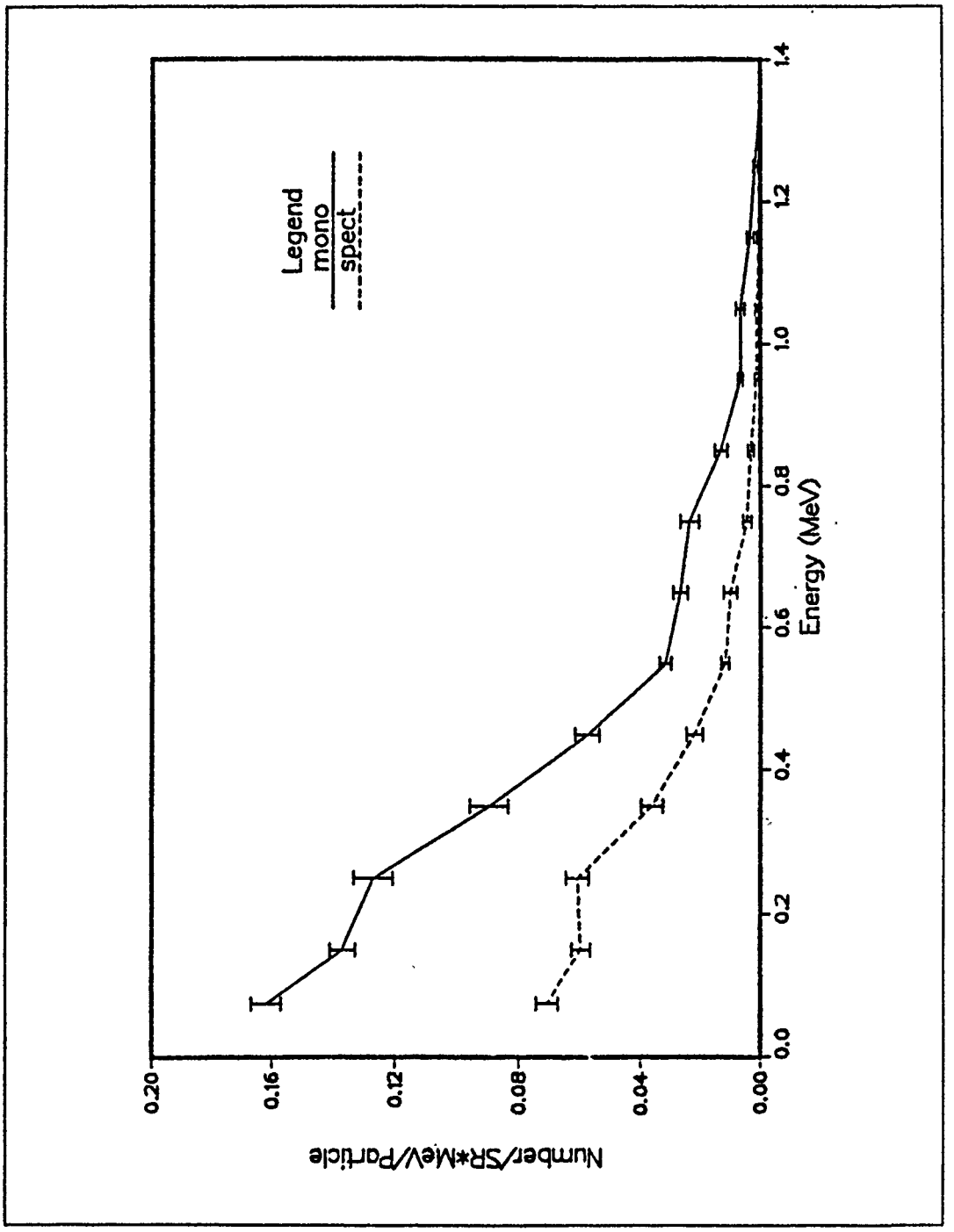

Figure 11. Transmitted Photon Energy Spectra for monoenergetic electron beam and spectrum source beam at a Marx charge of 75 kV

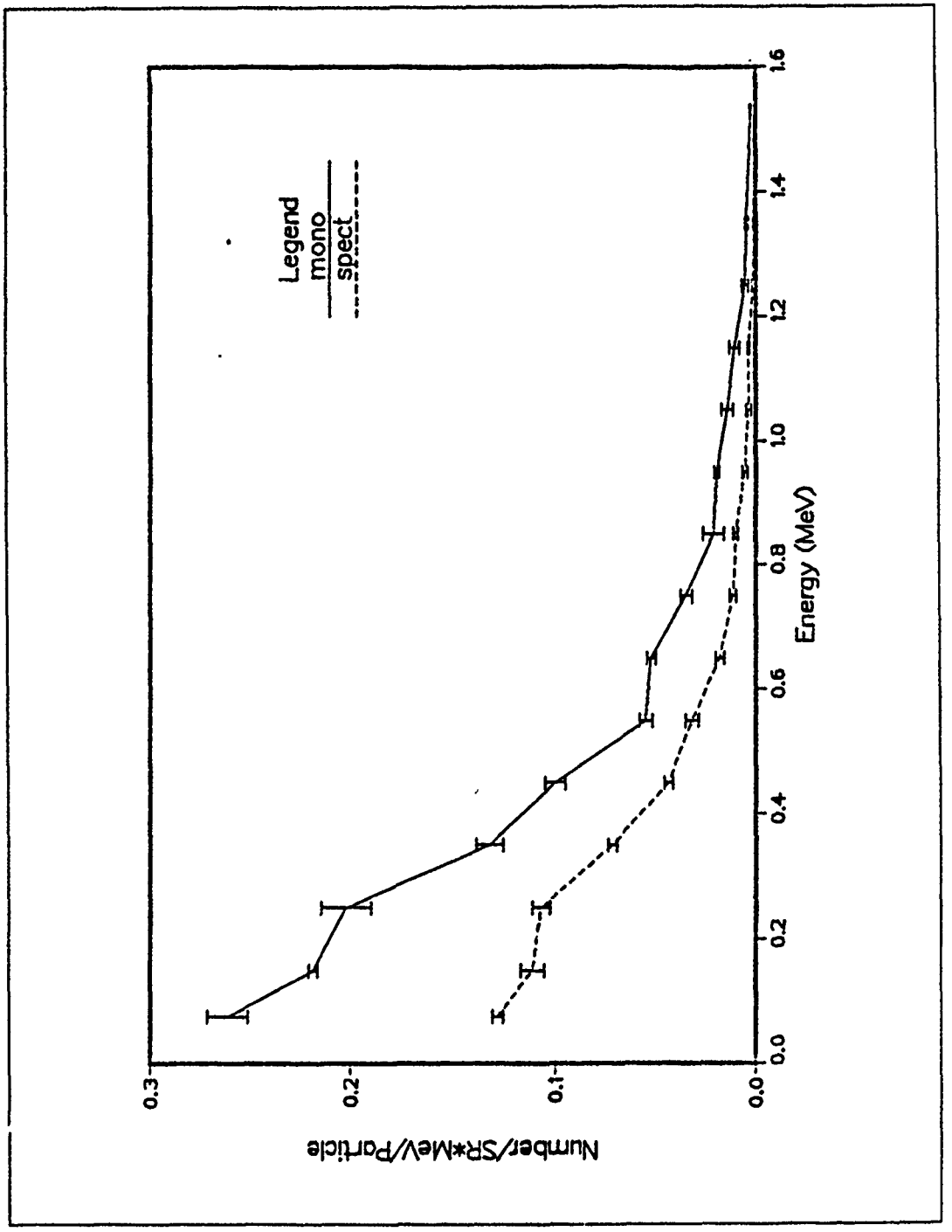

Figure 12. . Transmitted Photon Energy Spectra for Monoenergetic electron Beam and Spectrum Source at a Marx Charge of 100 kV

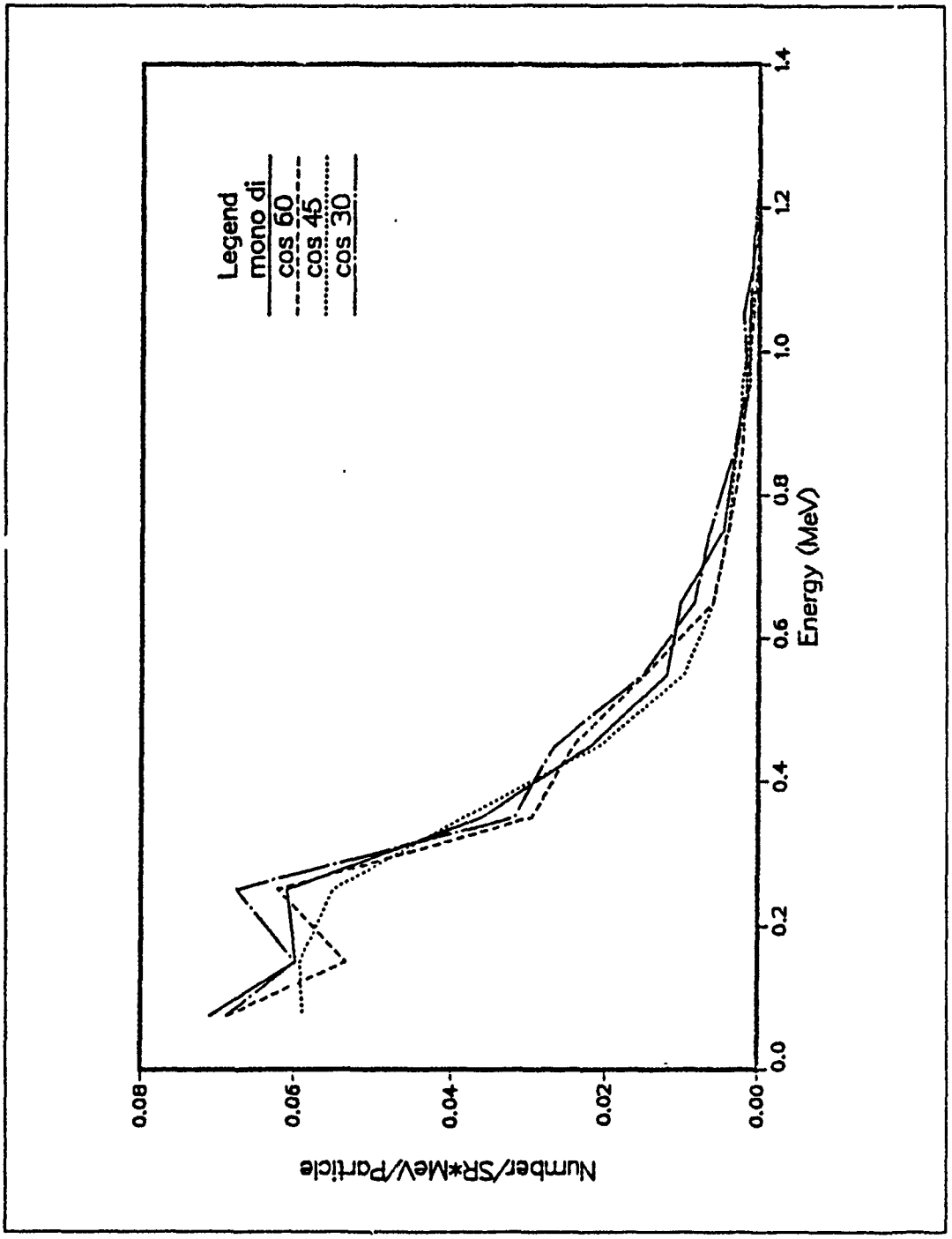

Figure 13. Transmitted Photon Energy Spectra for Spectrum Source Beam Having Different Angular Distribution(cosine law) at a Mmarx Charge of 75 kV

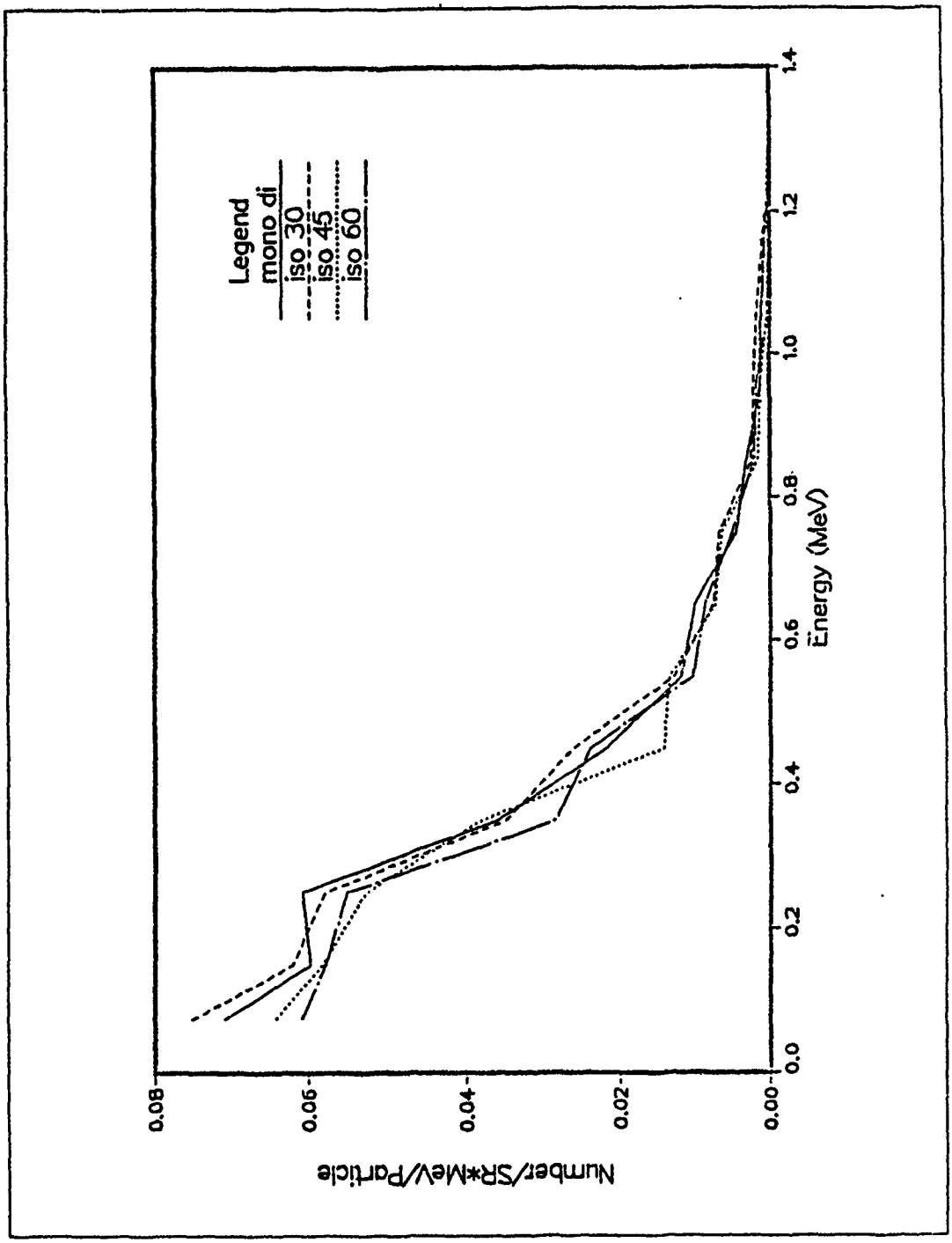

Figure 14. Transmitted Photon Energy Spectra for Spectrum Source Having Different Angular Distribution(isotropic) at a Marx Charge of 75 kV

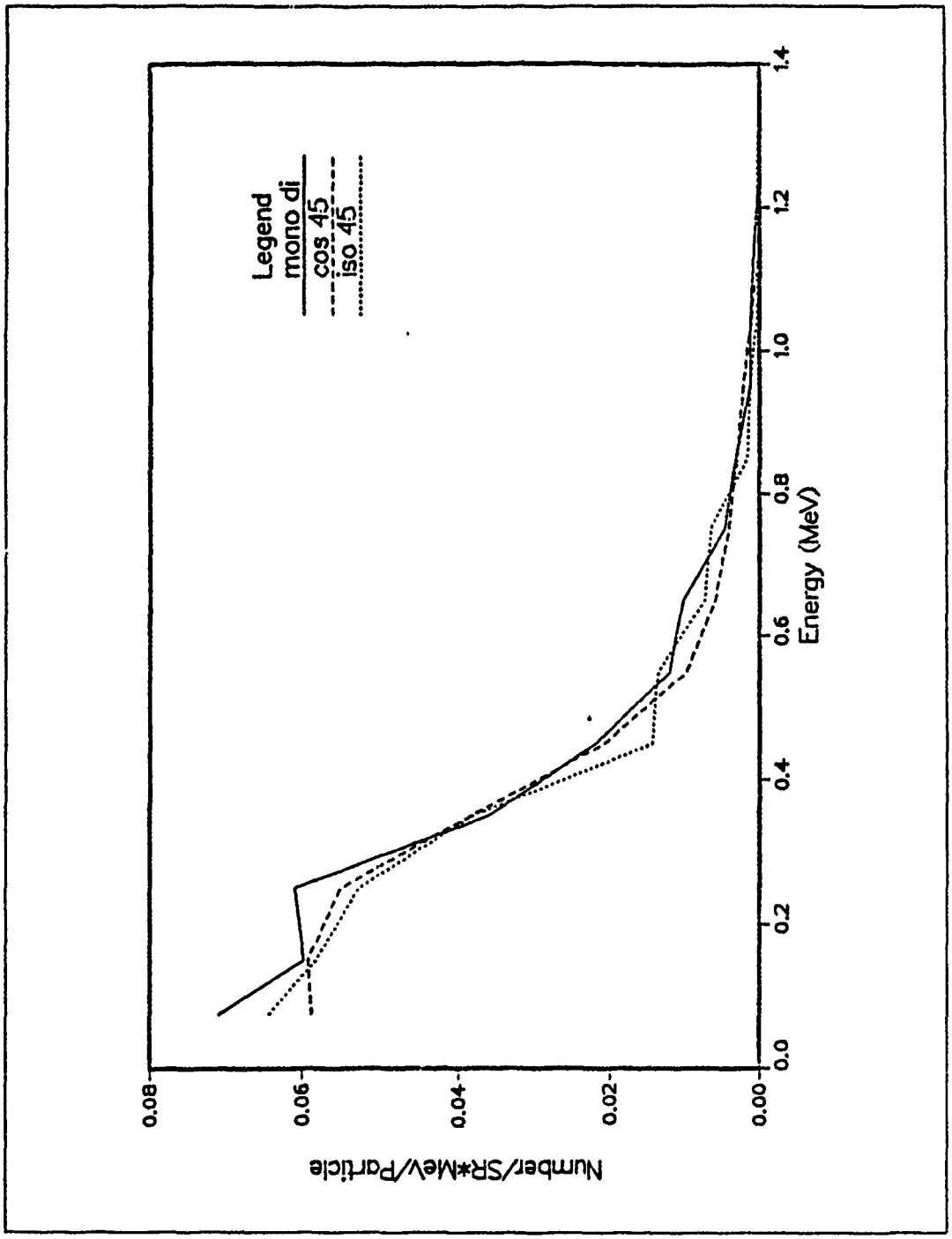

Figure 15. Transmitted Photon Energy Spectra for Spectrum Source Beam Having Cosine–law distribution and Isotropic Disrrbution at the Marx Charge of 75 kV.

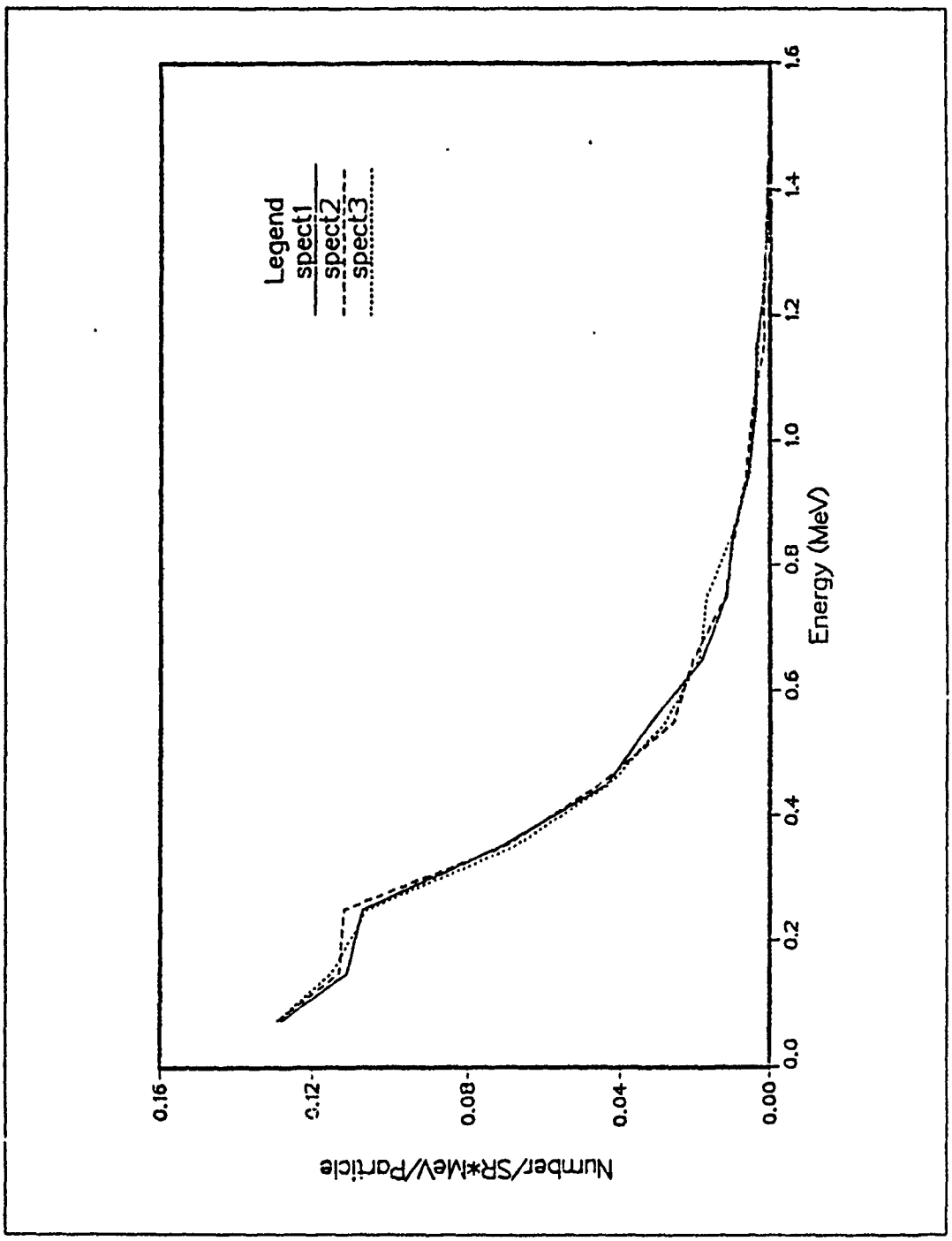

Figure 16. Transmitted Photon Energy Spectra for Different Cathode Radii at 75 kV Marx Charge (spect1; 1.8575 cm, spect2; 2.54cm, spect3; 3.81 cm)

C. INVESTIGATION OF THE ELECTRON SOURCE BEAM PARAMETERS

For the further analysis of the radiation output of the Model 112A x–ray generator, the unknown parameters of the electron source beam should be specified. Since the ITS/CYLTRAN codes can calculate the absorbed dose in the test material CaF_2:Mn, the radiation dosage patterns at the anode faceplate can be extracted. By comparing the measured exposure pattern with the simulated dosage patterns of ITS/CYLTRAN output, electron source beam parameters which are difficult to obtain by direct measurement can be determined.

1. CYLTRAN Input Parameters

The following three beam parameters are the major factors to be specified.

(a). the electron source beam radius(effective cathode radius)

(b). the angle of the dominant electron flow

(c). the peak energy of the electron source beam(or the peak current of the electron flow)

All the other input data are the same as those entered in previous section A (see Table VIII) and various values of the above three parameters are entered. The modeled configuration of the electron accelerator tube for the calculation of the radiation pattern in the test material is depicted in Figure 17. The TLD is divided into 10 spherical shell "zones" to have the radial dosage pattern. In order to get the closest simulation results a 'trial and error' method was applied in entering the input parameters.

If the absorbed dose in air, D_{air}, can be calculated directly by CYLTRAN, then the comparison is easy and the calculated exposure is obtained by the simple relation (1) in chapter II. Within a single Monte Carlo calculation, however, it is difficult to include both the generation of photons in the target and subsequent energy deposition from those photons in the small volume of air. The difficulty is caused by the low photon conversion efficiency for the electrons in the energy range considered here and by the low probability for photon interaction in small volume of air [Ref. 13]. Since this is also true for the test material CaF_2:Mn, the thickness of TLD was enlarged for the simulation input. The actual thickness of TLD in the experiment was 0.035 inch (0.089 cm). However, a thickness of 0.5 cm CaF_2:Mn was modeled in CYLTRAN.

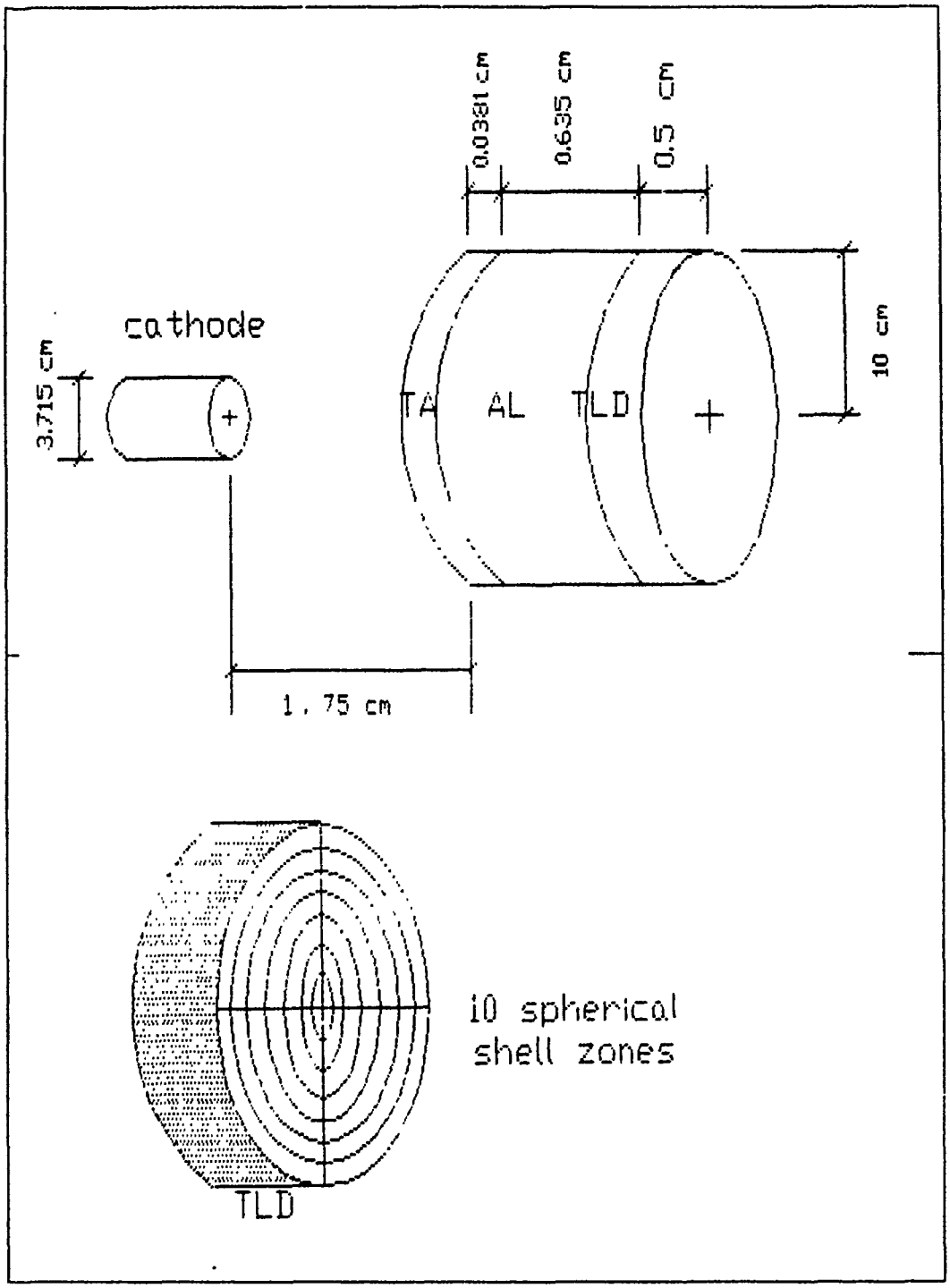

Figure 17. Geometry Configuration entered into CYLTRAN for Calculation of Absorbed Dose in TLD's.

2. 75 kV Marx Charge Series

a. Development of Dip at the Faceplate

One of the unexplained characteristics of the measured exposure pattern is that it has a dip at the geometric center of the anode faceplate. The simulated output of the ITS/CYLTRAN also has the same pattern at a specific angle of the dominant electron flow. For a Marx charge of 75 kV, Figure 18 shows the absorbed dose in TLD normalized to one incident electron at different source beam flow angles using the cosine–law distribution. The radius of the cathode in this case was 2.54 cm. At cosine–law 30, 45 and 60 degrees the dip appears at center and the pattern is similar to the measured exposure pattern. Cosine–law 45 degree simulation shows the most extreme dip pattern. The source beam distribution of cosine–law 60 was the most probable configuration when compared to the normalized patterns. The calculation was normalized, as will be explained in the section B, by dividing the calculated and measured absorbed dose by the maximum value. For various beam radii of the cosine–law 60.0 degree distributions, the dosage patterns were compared with each other in Figure 19. The cases of isotropic distribution of the electron source beam were also simulated and the characteristic center 'dip' did not show up (see Figure 20). In Figures 18, 19 and 20, the integration of the dosage throughout the whole distance is not constant. The dosage patterns in the anode (Ta converter and Al absorber) do not show a dip, but the characteristic dip appears in the TLD's chip. Figure 21 presents the development of a dip through the anode.

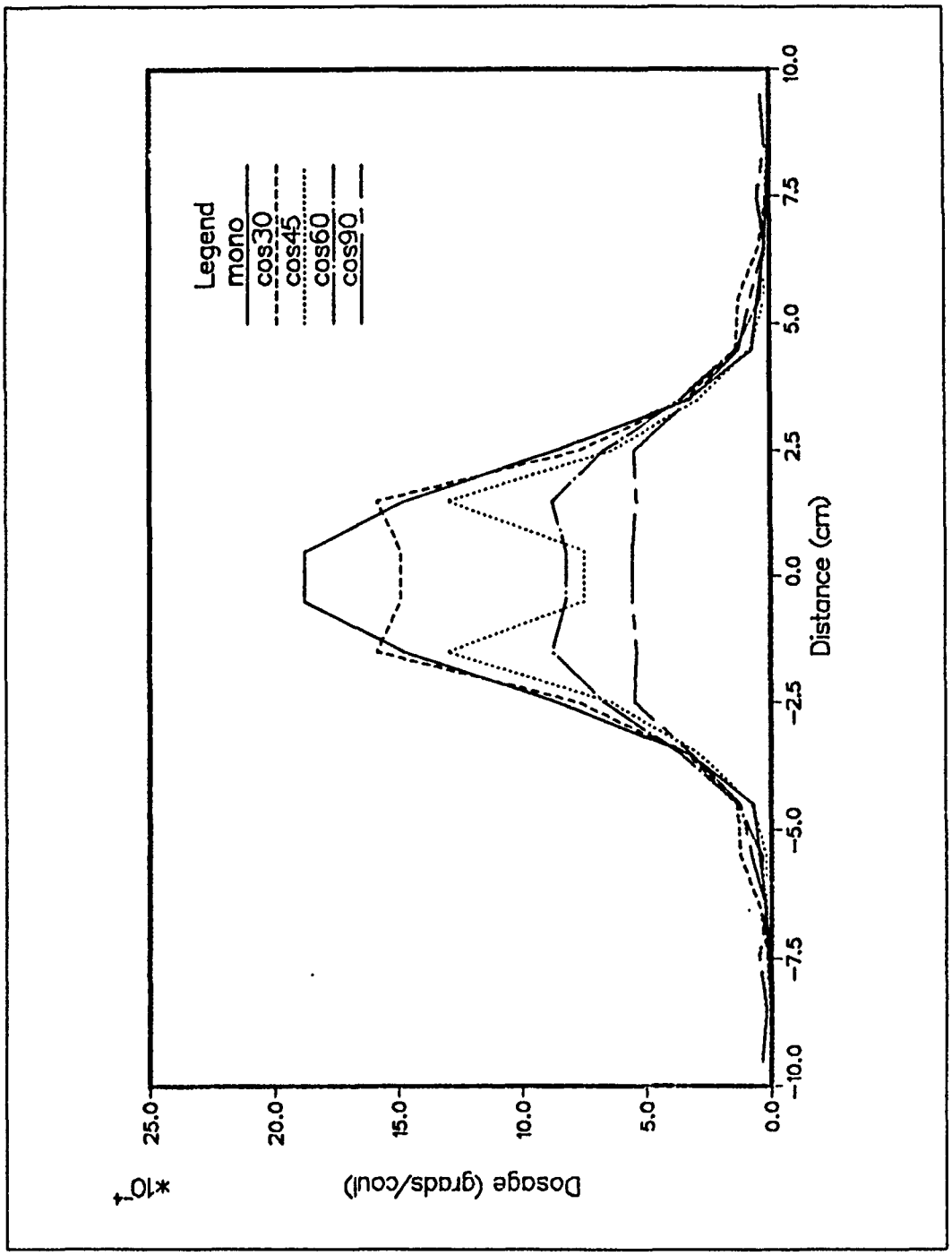

Figure 18. Radiation Dosage Pattern in TLD's for Different Source Beam Distribution (cosine–law) with a Marx Charge of 75 kV(normalized to one incident electron) The beam radius is 2.54 cm

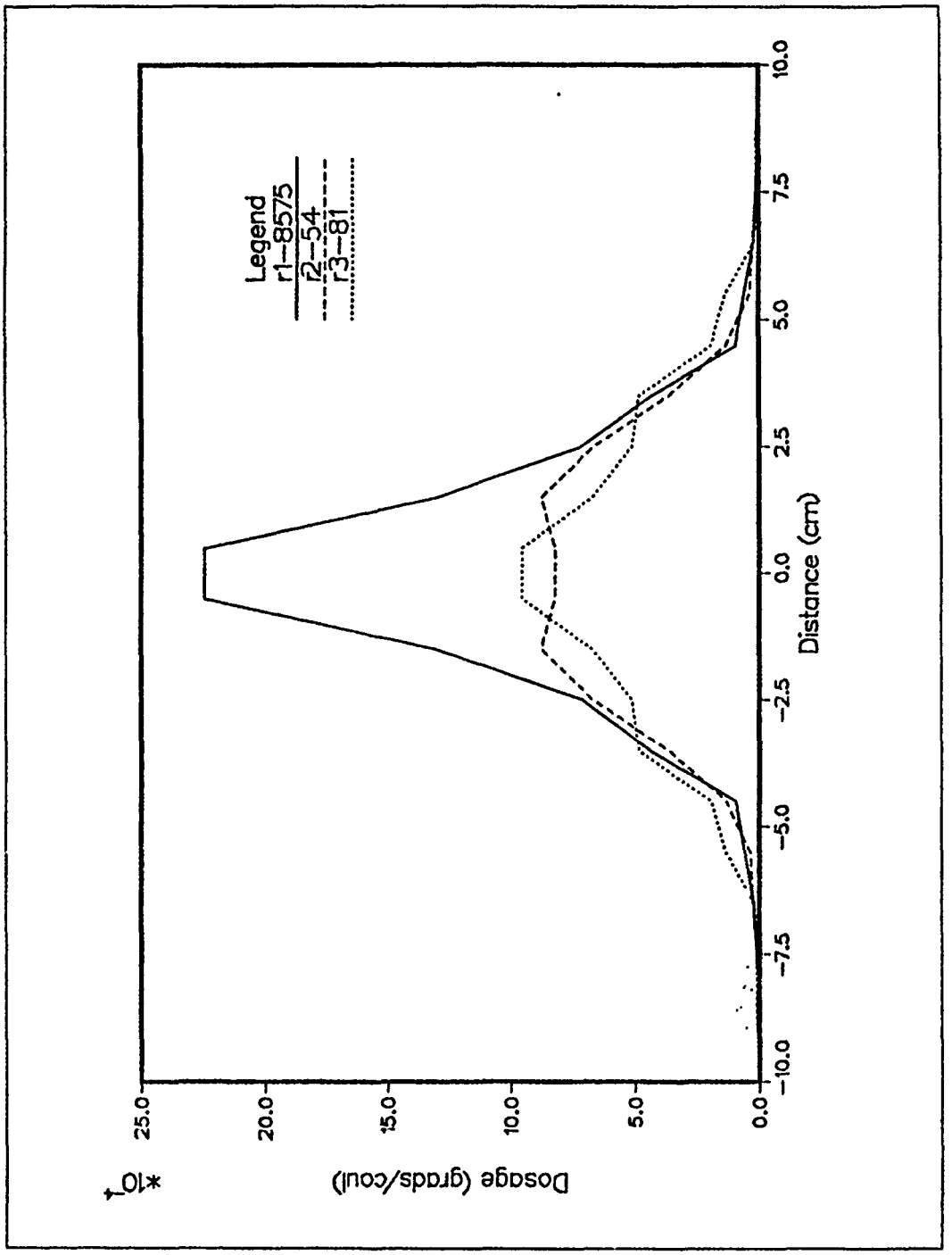

Figure 19. Radiation Dosage Pattern in TLD's for Different Source Beam Radii(1.86cm, 2.54cm and 3.81cm) and for the Cosine–law 60 degree Beam Distribution with a Marx Charge of 75 kV(normalized to one incident electron)

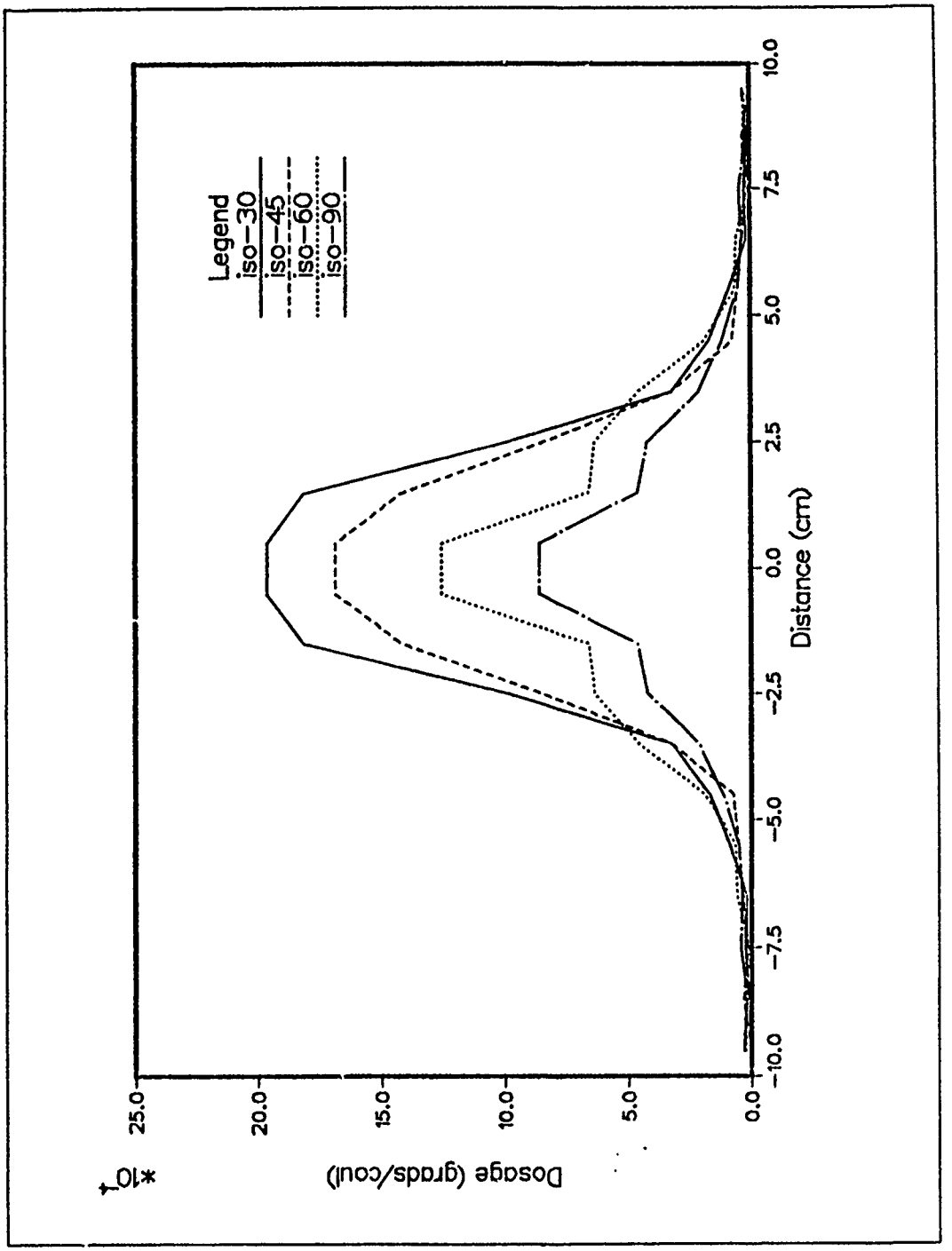

Figure 20. Radiation Dosage Pattern in TLD's for Different Source Beam Distribution (isotropic) with a Marx Charge of 75 kV(normalized to one incident electron) The beam radius is 2.54 cm

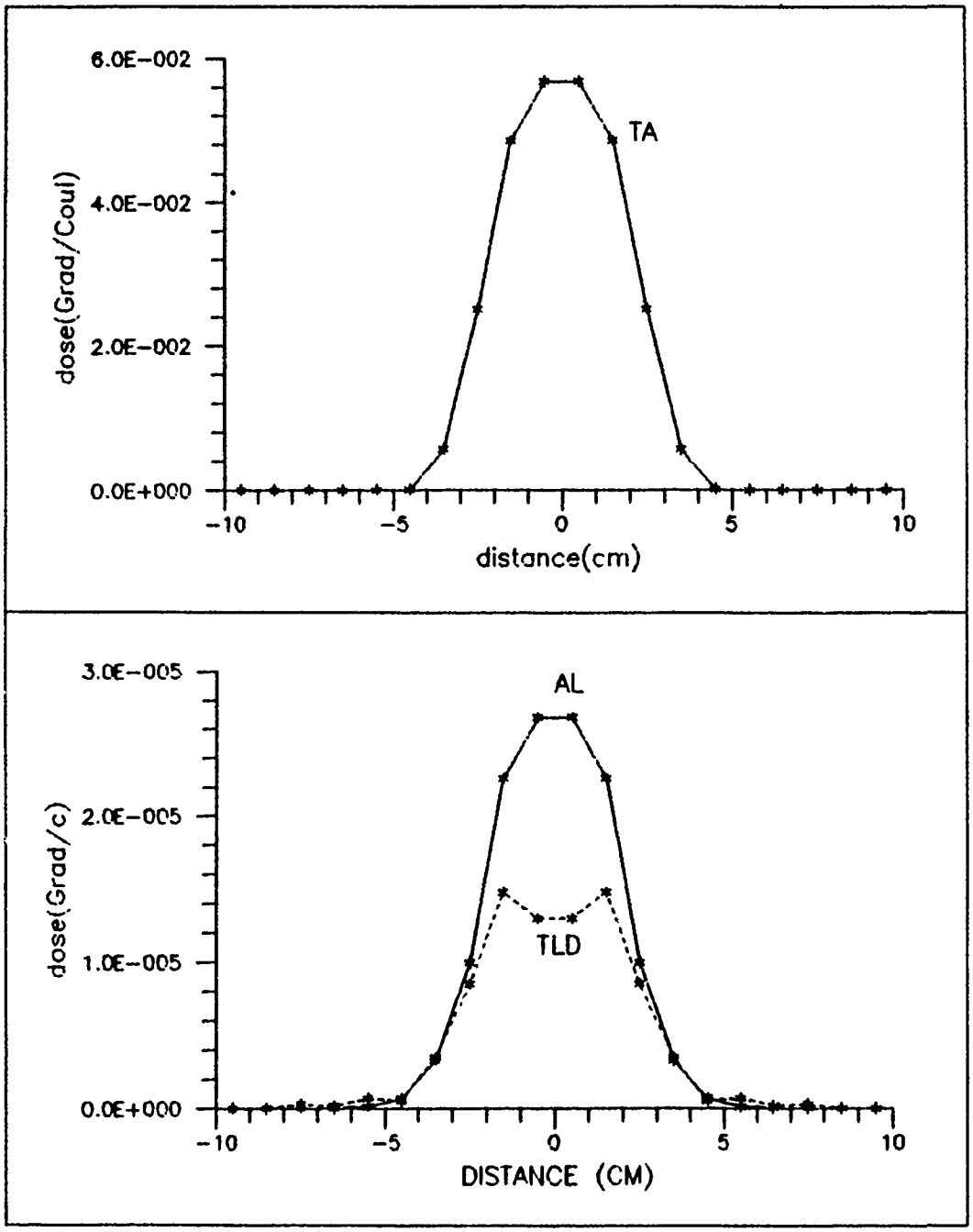

Figure 21. Radiation Dosage Pattern in TA(upper) and in AL and TLD (lower) for the Cosine–law 60 degree Beam Distribution with a Marx Charge of 75 kV (normalized to one incident electron)

b. Output and Comparison

In order to compare the simulated absorbed dose which is directly obtained by running CYLTRAN with the measured exposure which is obtained from the experiment, the exposure values measured should be converted to absorbed dose values in the test material. The procedures for calculation of the absorbed dose from the measured exposure were followed as explained in Chapter II. The photon energy fluence in each zone obtained by CYLTRAN in terms of "photon flux distribution (track–length/Voi–MeV–particle)" at 75 kV Marx charge is presented in Table XI. Since the absorbed dose in TLD calculated by CYLTRAN is normalized to one incident electron, these computed absorbed dose also have to be converted to absorbed dose for the each electron propagating during the pulse. From the current wave form taken during the experiment (see Figure 7 and Figure 8), the number of electrons can be obtained by integrating the current for the duration of pulse.

Large difference between the absorbed dose converted from the experimental exposures averaged and the absorbed dose calculated by CYLTRAN were observed. This comparison is shown in Figure 22. The calculated absorbed dose is factor of 2 to 5 times smaller than the measured absorbed dose. There may be some experimental reasons for this large difference. One possible reason would be that the operation time was more than the 20 nsec specified in the operations and maintenance manual. Since the system is based upon time–dependent electrical breakdown, the longer switch time may result in higher radiation output. Another error source may be the unshielded TLD's used during the experiments. Unshielded dosimeters do not provide electron equilibrium in a high energy gamma field. The

ratio of the indicated exposure and actual exposure in pressed chip TLD's ranges from 2 to 10 [Ref. 7]. So unshielded TLD's may result in higher exposures than actual exposures. For this reason the measurements of Reference 1 should be repeated using shielded doimeters.

Because there was such significant difference between the CYLTRAN results and the measured absorbed dose, a normalized dosage pattern was produced. This normalization was performed by dividing each absorbed dose by the maximum values so that the dosage patterns could be compared. The consequences of this normalization are depicted graphically in Figure 23, which compares the experimental results and CYLTRAN outputs.

From these comparisons the possible source beam parameters, which were entered and produced the closest radiation dosage pattern to the experimental results, are summarized in the following table.

TABLE VIII : SOURCE BEAM PARAMETERS
(produced the most similar dosage pattern to experimental result at the Marx charge of 75 kV)

	Simulation Input
Beam Radius	2.54 cm
Electron Flow	cosine–law 60^{0}
Source Energy Spectrum	peak energy 1.34 MeV

TABLE VIIII : PHOTON FLUENCE IN EACH ZONE AT 75 KV MARX CHARGE FOR COSINE–LAW 60 DISRIBUTION AND 2.54 CM BEAM RADIUS(track–length/Vol–MeV, normalized to one incident electron)

	zones							
energy (MeV)	"1"	"2"	"3"	"4"	"5"	"6"	"7"	"8"
1.4	0.0	0.0	0.0	0.0	0.0	0.0	0.0	0.0
1.3	0.0	0.0	0.0	0.0	0.0	0.0	0.0	0.0
1.2	0.0	0.0	0.0	0.0	0.0	0.0	0.0	0.0
1.1	1.28E–4	4.25E–5	0.0	0.0	0.0	0.0	0.0	0.0
1.0	8.18E–5	0.0	0.0	1.19E–5	0.0	1.24E–5	1.29E–5	5.84E–6
0.9	8.20E–5	7.34E–5	2.10E–5	0.0	0.0	0.0	0.0	0.0
0.8	0.0	6.71E–5	1.03E–4	0.0	8.58E–6	1.54E–5	0.0	0.0
0.7	1.83E–4	1.93E–4	1.88E–4	1.07E–4	2.70E–5	1.60E–5	7.49E–6	0.0
0.6	1.59E–4	4.35E–4	9.66E–5	2.15E–4	1.25E–4	7.30E–5	5.72E–6	1.16E–5
0.5	2.29E–4	6.49E–4	3.31E–4	1.13E–4	1.60E–4	4.15E–5	0.0	0.0
0.4	3.66E–4	5.48E–4	4.04E–4	2.95E–4	1.34E–4	2.60E–5	2.00E–5	4.19E–6
0.3	1.28E–3	8.65E–4	6.66E–4	3.96E–4	1.98E–4	1.02E–5	4.48E–5	1.75E–5
0.2	1.95E–3	2.08E–3	1.37E–3	9.11E–4	5.25E–4	1.60E–4	5.27E–5	1.16E–5
0.1	3.08E–3	3.04E–3	2.04E–3	1.01E–3	5.27E–4	2.04E–4	6.96E–5	4.70E–5
0.05	4.26E–3	1.90E–3	1.50E–3	8.41E–4	4.57E–4	1.07E–4	1.85E–5	5.17E–7

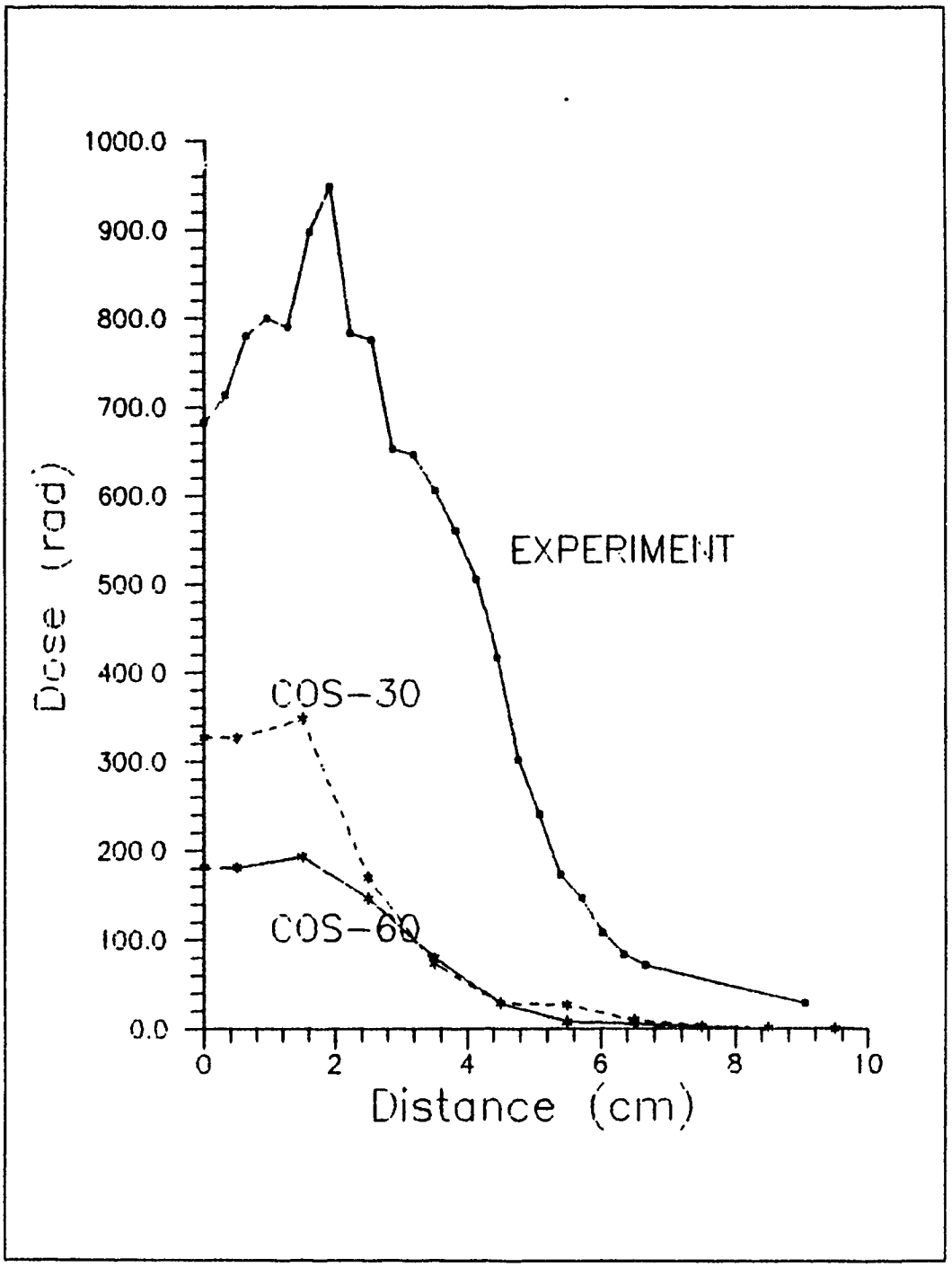

Figure 22. Comparison of the Absorbed Dose Between the CYLTRAN Outputs and Experimental Result at a Marx Charge of 75 kV

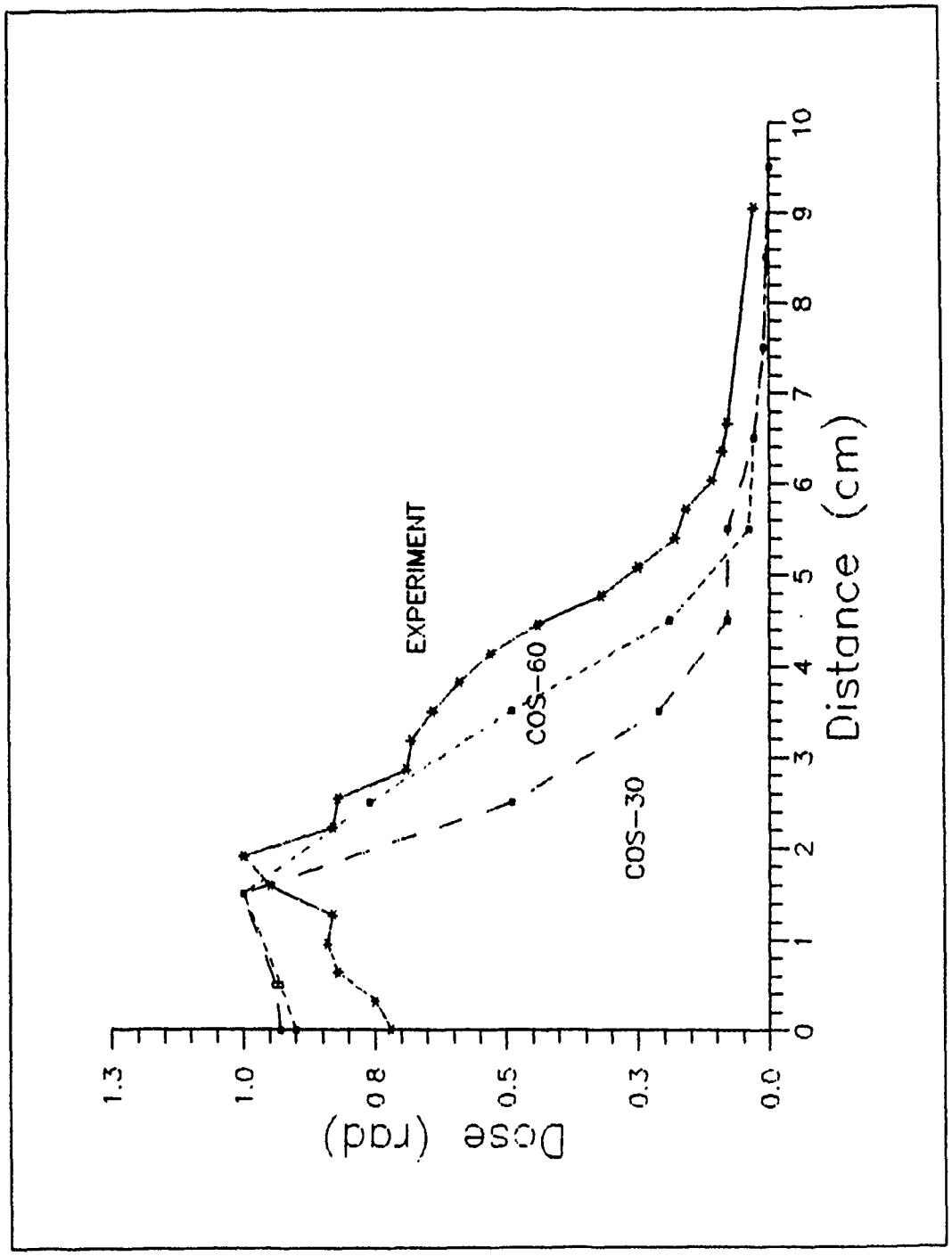

Figure 23. Comparison of the Dossage Patterns Normalized by the Maximum values at a Marx Charge of 75 kV

3. 100 kV Marx Charge Series

The same method of analysis and calculation procedures were used for the Marx charge of 100 kV to investigate the electron source beam parameters. The simulation input parameters given in table XII produced the most similar dosage pattern to the experimenatal results. The comparison between the CYLTRAN output and experimental result is presented in Figure 24. There is also a huge difference between them. The same normalization to the 100 kV series was done and compared with each other and presented in Figure 25.

TABLE X : SOURCE BEAM PARAMETERS
(produced the most similar dosage pattern to experimental result at the Marx charge of 100 kV)

	Simulation Input
bean radius	2.54 cm
electron flow	cosine–law 45^{0}
source energy spectrum	peak energy 1.66 MeV

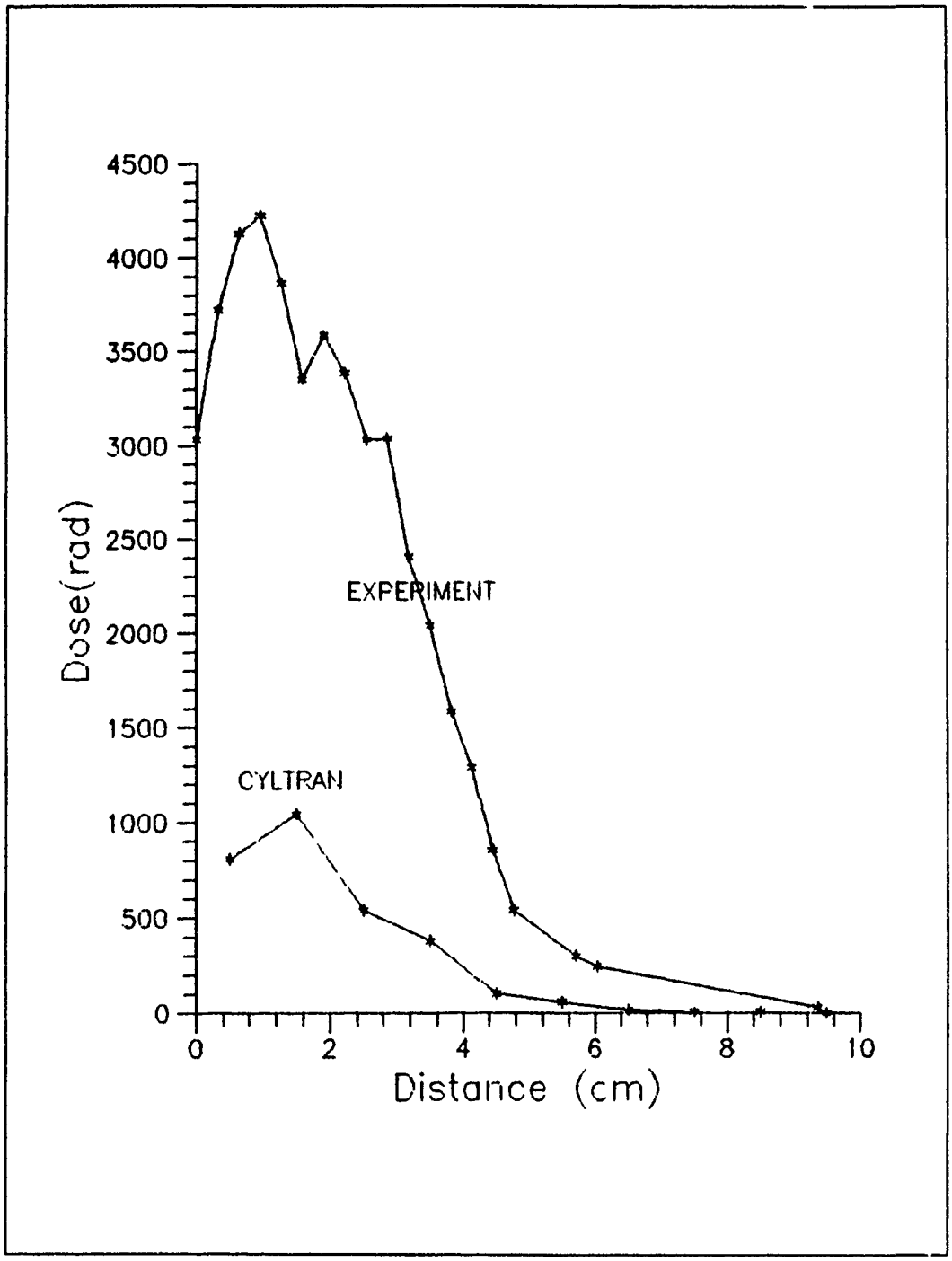

Figure 24. Comparison of the Absorbed Dose Between the CYLTRAN Outputs and Experimental Result at a Marx Charge of 100 kV

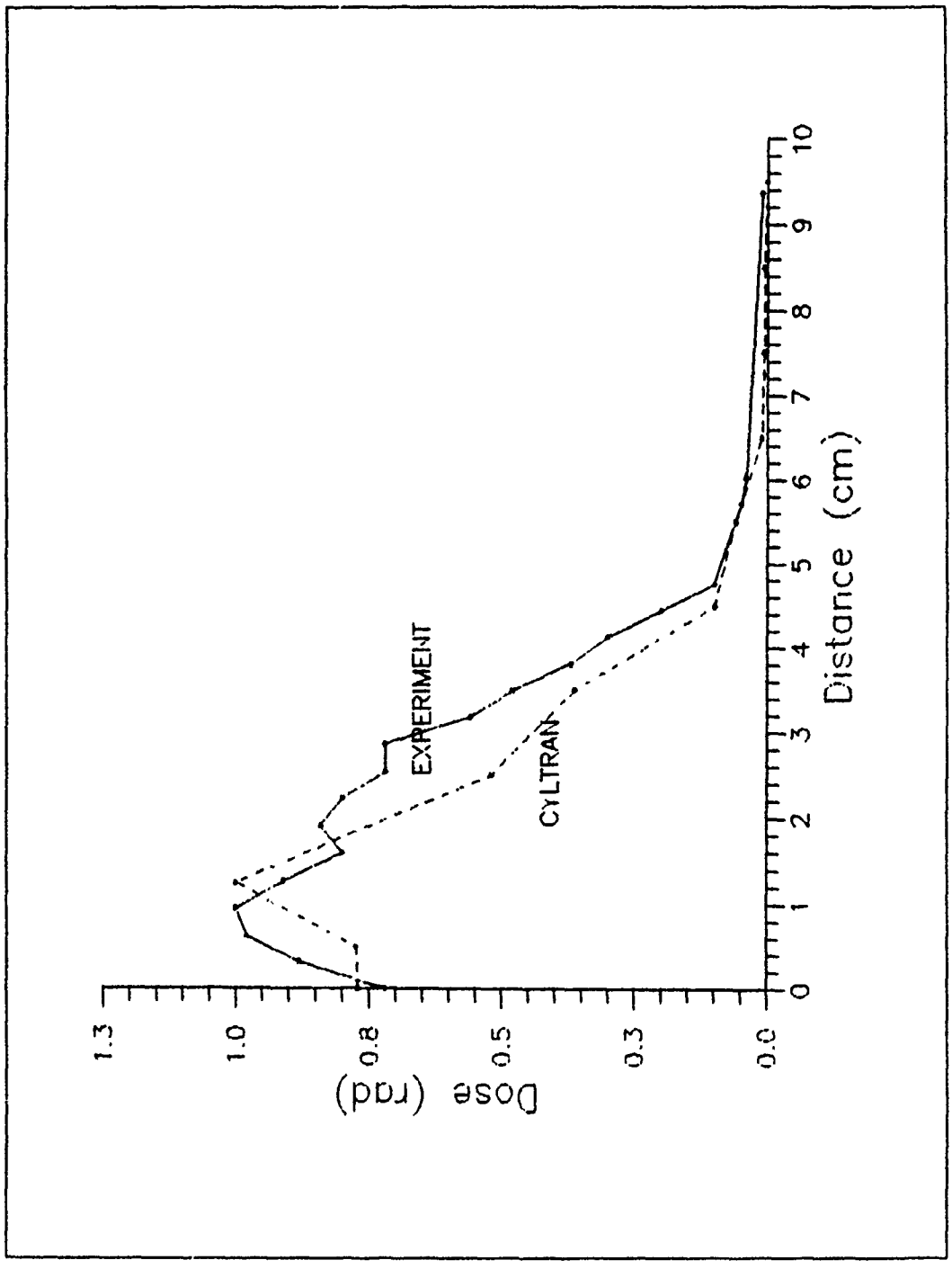

Figure 25. Comparison of the Dossage Patterns Normalized by the Maximum values at a Marx Charge of 100 KV

D. PREDICTION OF THE RADIATION DOSAGE

The design specifications of the Model 112A Pulserad Pulsed X–Ray Generator is provided in the following table as listed in the Operations and Maintenance Manual.

TABLE XI : SYSTEM SPECIFICATIONS

Marx Charge Voltage	100 kV
Output Voltage	1.7 MV
Pulse Width	20 ns
Exposure at 0.5 m from anode	8 roentgen

The same simulation input parameters of the electron source beam, as given in Table XII, were entered. The simulation model geometry is depicted in Figure 26. The AL equilibrator of 0.2 cm thickness was placed to establish Charged Particle Equilibrium (CPE). This equilibrium thickness is proper for our photon energy transmitted [Ref. 9]. Figure 27 shows the radiation pattern in TLD's in rad at the axial distance 0.5 m fron the anode assembly. The procedures in Chapter III were followed to convert the design dose specification in roentgen to the absorbed dose in rad in TLD's. in order to compare this design dose output with the CYLTRAN result. The comparison between the CYLTRAN output and the design dose output is presented in Table XIV, showing that they are in good agreement each other.

TABLE XII : DOSE COMPARISON BETWEEN CYLTRAN OUTPUT AND DESIGN SPECIFICATION (at the axial distance 50 cm from anode)

CYLTRAN output	Design dose
8.5 rad	8.2 rad

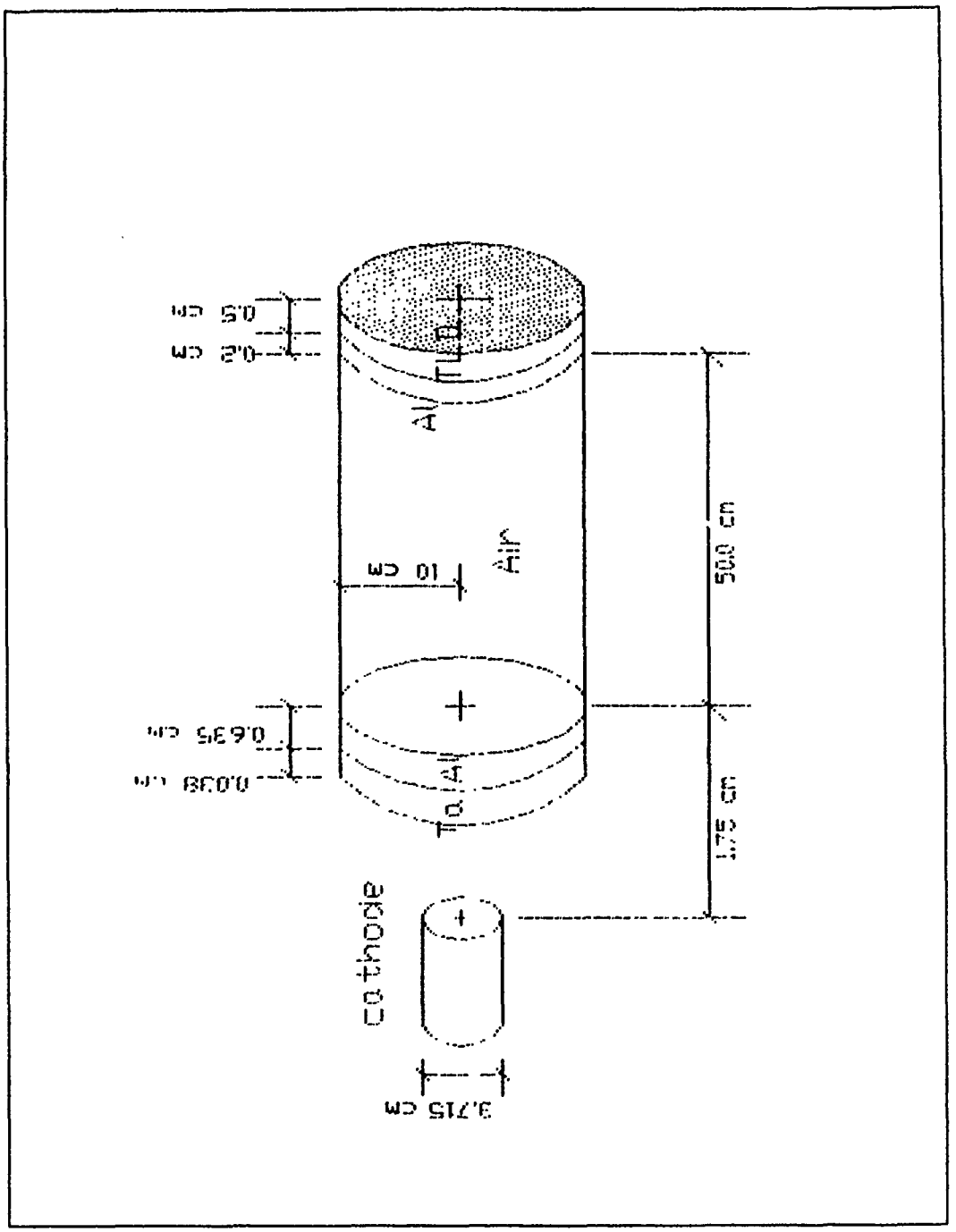

Figure 26. Geometry Configuration of CYLTRAN for Calculation of Absorbed Dose in TLD's at the axial distance 50 cm from anode

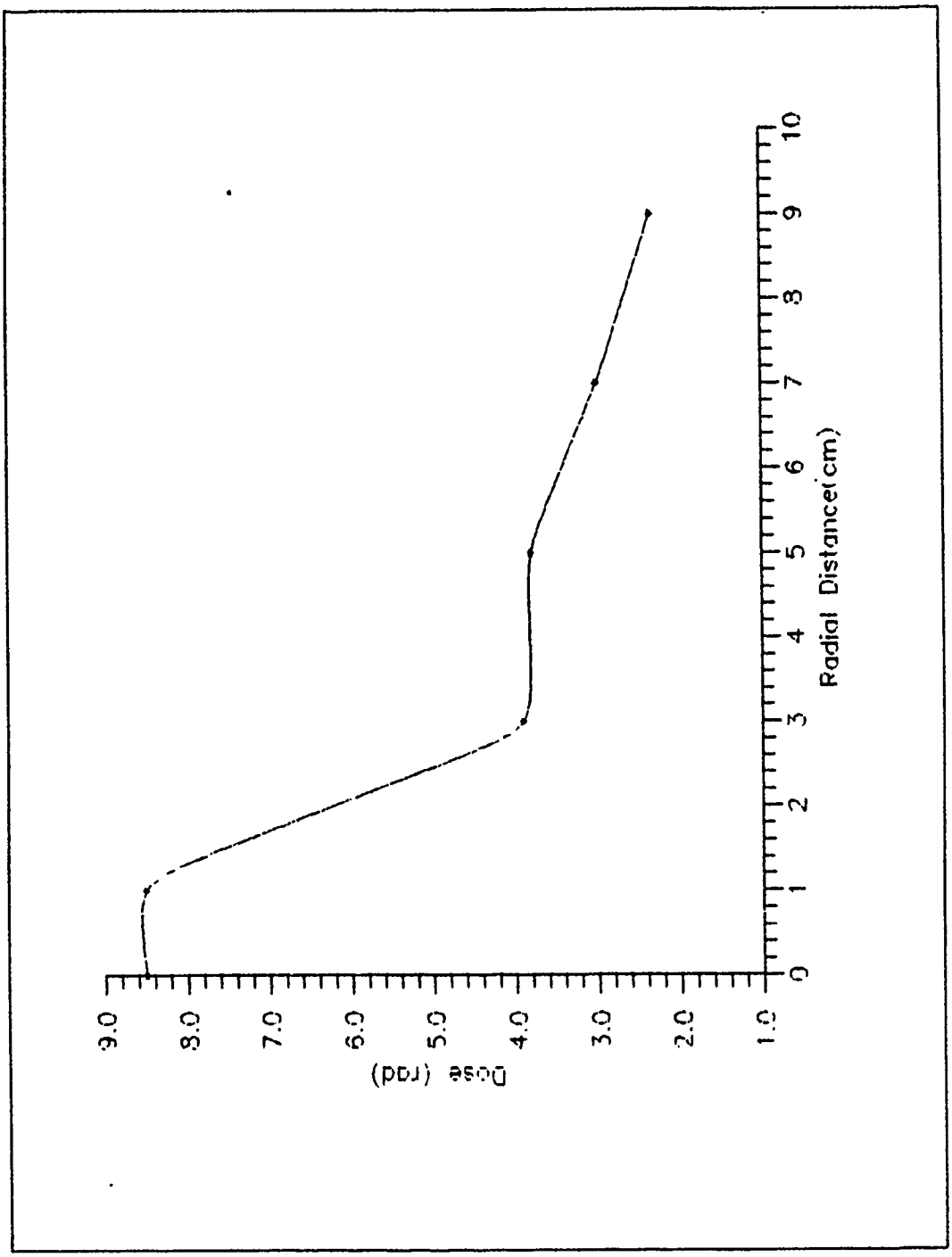

Figure 27. Calculated Absorbed Dose in TLD's at the Axial Distance 50 cm from anode

IV. CONCLUSIONS AND RECOMENDATIONS

The CYLTRAN simulation modeled for the Model 112A Pulsrad Pulsed X–ray Generator can be concluded as follows:

1. The overall photon energy spectrum transmitted from the x–ray machine is independent of the electron source beam parameters such as beam radius and electron angular distribution.
2. The source beam was found to have angular distribution of electrons, confined within 60 degrees and proportonal to the cosine of the angle with respect to the cathode center axis at a Marx charge of 75 kV and 45 degrees at 100 kV Marx charge.
3. The CYLTRAN calculations of the absorbed dose in TLD's were considerably smaller than the measured values at the anode faceplate.
4. However, the CYLTRAN output agreed with the design dose specification at the distance 50 cm from anode. This agreement may be an indication that the same code was used by the manufacturer.

To make effective use of the Pulserad 112A a experiment of measurement of the radiation dose with establishment of Charged Particle Equilibrium at the various axial distance is recommended. The experimental method is described in detail in Reference 9.

APPENDIX A. SAMPLE INPUT FILES

Sample input file to generate a cross section tape.

```
Energy 1.7
Material Ta
Material Al
Material Ca 0.495 F 0.484 Mn 0.021 Density 3.18
title
        1.7 MeV Cross Section for Ta, Al and CaF2:Mn
```

Sample Input File to excute ITS

```
Echo 1
Title
      Mat; Ta, Al, CaF2:Mn  His; 40000  Energy; 1.34(spectrum)
Spectrum 7
      1.0 0.643 0.439 0.246 0.096 0.032 0.0
      1.34 1.0 0.8 0.6 0.4 0.2 0.01
Cutoffs  0.05  0.05
Position  0.0  0.0  0.0
Radius  2.54
Direction  0.0  0.0
      Cosine–law  60.0
Geometry 4
      0.0          1.75         0.0   10.0   0
      1.75         1.7881       0.0   10.0   1   1   1   10
      1.7881       2.4231       0.0   10.0   2   1   1   10
      2.4231       2.9231       0.0   10.0   3   1   1   10
Electron–escape
      Nbine 15 user
      1.4 1.3 1.2 1.1 1.0 0.9 0.8 0.7 0.6 0.5 0.4 0.3 0.2 0.1 0.01
      Nbint 15 user
      1. 2. 3. 5. 7. 10. 13. 16. 20. 30. 45. 60. 75. 90. 180.
Photon–escape
      Nbine 15 user
      1.4 1.3 1.2 1.1 1.0 0.9 0.8 0.7 0.6 0.5 0.4 0.3 0.2 0.1 0.01
  Nbint 15 user
      1. 2. 3. 5. 7. 10. 13. 16. 20. 30. 45. 60. 75. 90. 180.
Photon–flux  22 31
      Nbine 15 user
      1.4 1.3 1.2 1.1 1.0 0.9 0.8 0.7 0.6 0.5 0.4 0.3 0.2 0.1 0.01
Pulse–height 22 31
      Nbine 15 user
      1.4 1.3 1.2 1.1 1.0 0.9 0.8 0.7 0.6 0.5 0.4 0.3 0.2 0.1 0.01
Histories  40000
```

APPENDIX B

MASS ENERGY–ABSORPTION COEFFICIENTS μ_{en}/ρ (cm^2/g) FOR VARIOUS MEDIA [Ref. 5]

Photon Energy	Air	CaF_2:Mn
0.01	4.61	51.7
0.015	1.27	16.1
0.02	0.511	6.86
0.03	0.148	2.03
0.04	0.0668	0.850
0.05	0.0406	0.436
0.06	0.0305	0.256
0.08	0.0243	0.118
0.10	0.0234	0.0697
0.15	0.0250	0.0397
0.2	0.0268	0.0317
0.3	0.0287	0.0296
0.4	0.0295	0.0295
0.5	0.0296	0.0293
0.6	0.0295	0.0290
0.8	0.0289	0.0281
1.0 MeV	0.0278	0.0270
1.5 MeV	0.0254	0.0247
2.0 MeV	0.0234	0.0229

Of importance in this table is the significant dependence on the low energy component. The cutoff energy of photon should be as low as possible in running the ITS/CYLTRAN codes.

APPENDIX C

DIAGRAM OF THE PULSERAD 112A ELECTRON ACCELERATOR TUBE

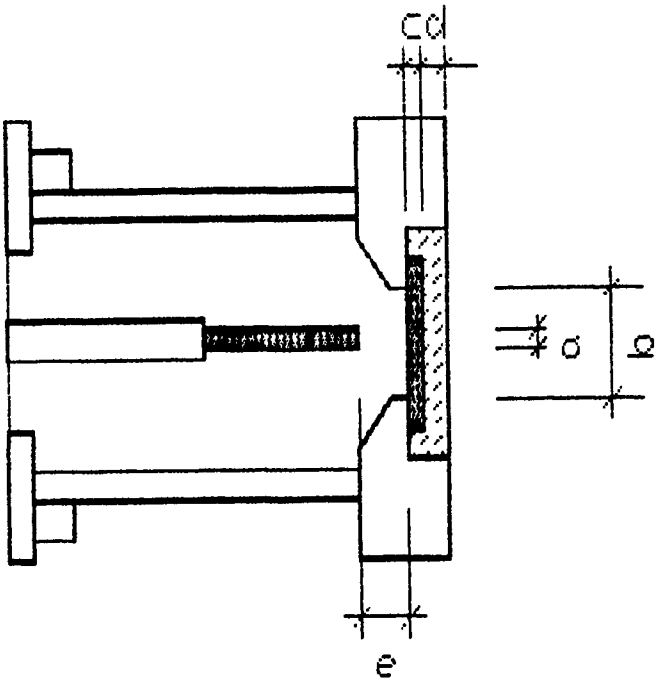

a = 1.86 cm
b = 10.16 cm
c = 0.0381 cm
d = 0.635 cm
e = 1.75 cm

APPENDIX D. TERMINOLOGY AND DEFINITION

A. EXPOSURE AND KERMA

Exposure is symbolized by X, and is defined as " the ionization equivalent of the collision kerma K_c in air, for x–ray and γ–rays." For monoenergetic photons K_c is related to the energy fluence Ψ by the mass energy–absorption coefficient $(\mu_{en} / \rho)_{E,Z}$

(1) $$K_c = \Psi \left(\frac{\mu_{en}}{\rho}\right)_{E,Z}$$

where

Ψ = energy fluence (J/cm^2)

μ_{en} = linear energy absorption coefficient (1/cm)

ρ = density (g/cm^2)

We can write that the exposure at a point due to an energy fluence Ψ of monoenergetic photons of energy E is given by

(2) $$X = \Psi \left(\frac{\mu_{en}}{\rho}\right)_{E,air} \left(\frac{e}{W}\right)_{air} = (K_c)_{air} / 33.97$$

where

X is the exposure in C/kg

Ψ is expressed in J/m^2

$(\mu_{en}/\rho)_{E,air}$ is in m^2/kg

$(e/\overline{W})_{air} = (1 / 33.97)$ C/J

The roentgen (R) is customary unit of exposure. It is converted by

$$X\ (C/kg) = 2.580 \times 10^{-4}\ X\ (R)$$

$$X\ (R) = 3876\ X\ (C/kg)$$

If a spectrum of photon energies $\Psi'(E)$ (in j/m^2–keV) is present at the point of interest P, and if $(\mu_{en}/\rho)_{E,air}$ (in m^2/kg) is the energy–absorption coefficient as a function of photon energy E for air, then the exposure at P will be given by

$$(3) \qquad X = \int_{E=0}^{Emax} (\mu_{en}/\rho)_{E,air}\ (e/\overline{W})_{air}\ \Psi'(E)\ dE$$

where

$(e/\overline{W})_{air} = (1/33.97)$ C/J

$\Psi'(E)$ = distribution in photon energy fluence; $J/(cn^2$–keV)

dE is in keV

X is in C/kg

B. ABSORBED DOSE AND KERMA

The absorbed dose (D) is the quotient of $d\epsilon$ by dm, where $d\epsilon$ is the mean energy imparted by ionizing radiation to matter of mass dm. The unit for absorbed dose is the gray(Gy).

$$1 \text{ rad} = 10^{-2} \text{ J/Kg} = 10^{-2} \text{ Gy}$$

The absorbed dose represents the energy per unit mass that remains in the material

The establishment of " charged particle equilibrium (CPE) " enables us to relate " absorbed dose " to " kerma". Under conditions of CPE, the absorbed dose is directly determined by the measurement of collision kerma.[Ref. 5]

$$(4) \qquad D_{air} = (K_c)_{air} = 0.876\ X \quad (\text{for CPE})$$

where $(K_c)_{air}$ and D_{air} are in rads, and X in roentgens.

Moreover, if the same photon energy fluence Ψ is present in media A and B having two different average energy absorption coefficients $(\mu_{en}/\rho)_a$ and $(\mu_{en}/\rho)_b$, the ratio of the absorbed doses under CPE conditions in the two media will be given by

$$(5) \qquad \frac{D_a}{D_b} = \frac{(K_c)_a}{(K_c)_b} = \frac{\overline{(\mu_{en}/\rho)_a}}{\overline{(\mu_{en}/\rho)_b}} \qquad (\text{for CPE})$$

where

$\overline{(\mu_{en}/\rho)_a}$ and $\overline{(\mu_{en}/\rho)_b}$; average energy absorption coefficients

C. CHARGED PARTICLE EQUILIBRIUM

The formal definition of CPE is "a condition that exists in a material under irradiation if the energies, number, and direction of charged particles induced by the radiation are constant throughout the volume of interest, Therefore, within such a volume, the sum of energies of all charged particles entering it is equal to the corresponding sum for all particles leaving it."

To understand the charged particle equilibrium (CPE), consider a small volume of material, a mass of Δm. Let this volume of material be traversed by a beam of ionizing radiation. The absorbed dose in the material is by definition

$$\Delta D = \frac{\Delta E_D}{\Delta m}$$

where

$\Delta E_D = \Delta E_E - \Delta E_L$; the energy deposited in the material

ΔE_E, ΔE_L ; the energy entering and leaving the material during some time interval

In the case of incident photon radiation only the energy transfer to matter is a two step process:

1. Photons impart energy to electrons via the photoelectric, compton scattering, and pair production processes.

2. Electrons impart energy to matter via excitation, ionization, and elastic scattering processes.

Since the energy deposition process involves only photons and electrons, the energy deposited can be redefined as

$$\Delta E_D = [\Delta E_E(\gamma) + \Delta E_E(e)] - [\Delta E_L(\gamma) + \Delta E_L(e)]$$

where γ and e refers to photons and electrons respectively.

However, by definition, CPE exists when the energy carried into the mass by electrons equals the energy carried out of the mass by electrons. Hence,

$$\Delta E_D = \Delta E_E(\gamma) - \Delta E_L(\gamma) \qquad \text{(for CPE)}$$

The so–called equilibrium dose is then the ionization energy deposited in the material per unit mass

$$D_{eq} = \frac{\Delta E_E(\gamma) - \Delta E_L(\gamma)}{\Delta m}$$

This expression for the equilibrium dose is equivalent to the definition of collision kerma.[Ref. 7]

APPENDIX E. ITS/CYLTRAN CODE SYSTEM

The TIGER series of time–independent coupled electron–photon Monte Carlo transport codes is a group of multimaterial and multidimensional codes designed to provide a state–of–the–art description of the production and transport of the electron–photon cascade. All the codes are based primarily on the original ETRAN model which combines microscopic photon transport with a macroscopic random walk for electron transport. The basis of the ITS codes, ETRAN has been developed at the National Bureau of Standards.

A. ETRAN MONTE CARLO METHODS

The ETRAN model pertains only to schematization of the electron random walk that is used in the calculation. The methods used to generate electron trajectories go back to a paper published in 1963 [Ref. 8], and involve the sampling from relevant multiple scattering distributions. The code follows all generations of electrons and photons with energies up to 1 GeV and down to 1 keV in any target material. The result is a calculation which takes onto account primary electrons, positrons or photons,and all secondary radiations, including knock–on electrons from electron–impact ionization events, electron bremsstrahlung, Compton electrons, photoelectrons, electron–positron pairs, annihilation radiation, and K–shell characteristic x–rays and Auger electrons resulting from electron and photon ionization events.

1. Photon Transport

Successive photon interactions are sampled individually in direct analogy to the physical process. Compton scattering, photoelectric absorption and pair production are included. The cross sections for these interactions are taken from the work of Hubbel done and have been organized into a database with which the necessary computation can be rapidly performed for any material. The photon Monte Carlo procedure is as follows. The distance to the next photon interaction is sampled from an exponential distribution governed by the attenuation coefficient. Then the type of interaction is then sampled from the appropriate relative probabilities. The history of each photon is continued from collision to collision until the photon either absorbed, escapes the target, or its energy falls below a chosen cutoff value.[Ref.6]

2. Electron Transport

The step pathlengths in ETRAN are chosen on two levels. First, major steps are defined such that, on the average, the kinetic energy of the electron is reduced by a constant factor. Then the major steps are divided into several equal–length sub–steps in order to keep the mean deflection angle small, which is required for applying the multiple–scattering theory. At the end of each sub–step the angular deflections are sampled. The net angular deflection from the combined effect of the elastic and inelastic collisions in a single sub–step is sampled from the Goudsmit–Saunderson multiple–scattering distribution.

The energy loss due to multiple ionization and excitation collisions in a pathlength is described by the Landau distribution which is corrected by Blunk and Leisagang. In ETRAN, the collision energy loss for each major step is sampled from the Landau/Blunck–Leisegang distribution. The radiative energy loss for the

electron is determined by sampling the production of bremsstrahlung photons using a dataset of bremsstrahlung production cross sections developed by M. J. Berger and S. M. Seltzer.

The production of knock–on electrons, whose energies are above a chosen cutoff value, is sampled according to the Moller cross section for collisions between free electrons. K–shell ionization events in each sub–step are sampled on the basis of Kolbenstvedt's cross section and either the emission of characteristic x–rays or Auger electrons are selected. For positron, most of the necessary cross–section information is available within the code, but separate sampling has not been implemented.

Electron histories are terminated under a variety of conditions. A maximum cutoff value is selected so that no electron histories is terminated at a higher energy unless it escapes the target. Another energy is selected to be the minimum cutoff value to have no electron flowed to a lower energy. At energies between these two cutoffs, the history is terminated if the residual range is smaller than the distance to nearest boundary.[Ref.6]

B. ITS CODE SYSTEM

ITS is a powerful and user–friendly software package permitting accurate Monte Carlo Solution of linear time–integrated coupled electron/photon radiation transport problems,with or without the presence of macroscopic electric and magnetic fields of arbitrary spatial dependence. The ITS code system consists of four essential elements:

XDATA	: The electron/photon cross section data file
XGEN	: The cross section generation program
ITS	: The Monte Carlo Program file
UPEML	: A machine portable update emulator

The heart of ITS is the Monte Carlo program file, which contains the eight codes of Table II. Each of eight member codes will run on any of four machines–CRAY, CDC, VAX, or IBM. The update emulator program UPEML creates the various Monte Carlo codes for given system with any corrections to those codes that may be desired. Program XGEN generates the problem specific cross section data tape using file XDATA for referenced inputs and a user defined input file. The Monte Carlo codes then read in the cross section tape and process the user defined problem.

TABLE XIII: ITS Member Codes

Standard Codes	Enhanced Ionization and Relaxation (P Codes)	Macroscopic Fields (M Codes)
TIGER	TIGERP	
CYLTRAN	CYLTRANP	CYLTRANM
ACCEPT	ACCEPTP	ACCEPTM

One of the eight ITS code is CYLTRAN, which simulates the transport of particle trajectories through a three–dimensional cylinder. Only the CYLTRAN code was used for this project. The following steps are required to execute a CYLTRAN run.

1. Generate a cross section tape based on the different type of materials contained in the cylindrical geometry of a problem
2. Create an input file which lists all the input parameters required to calculate desired outputs.
3. Submit the input file and the generated cross section tape to the ITS Monte Carlo codes to execute a run.

In addition to certain diagnostic information, the default output consists of:

1. Energy and number escape fractions (leakage) for electrons, unscattered photons and scattered photons.
2. Charge and Energy deposition profiles.
3. An explicit statement of energy conservation.

Theses data are sufficient to confirm the general partioning and conservation of charge and energy. In addition to the default output, a number of optional outputs may be selected through the use of the appropriate keywords. These are:

1. Escape fractions that are differential in energy for both electrons and scattered photons.

2. Escape fractions that are differential in angle for both electrons and scattered photons.
3. Coupled energy and angular distributions of escaping electrons and scattered photons.
4. Volume–averaged energy distributions of electron and photon scalar flux for selected regions of the problem geometry.
5. Pseudo–pulse–height distributions for selected regions of the problem geometry.(The key word pulse–height causes the spectrum of absorbed energy to be calculated for zones)

Except for an initial diagnostic table containing accounting information on the various particle types, every output quantity is followed by a one or two digit integer that is an estimate of one–sigma statistical uncertainty of that quantity expressed in percent.

C. COMPUTATION TIME

The computation time depends on the choices of run parameters of the problem considered. The sample input file specified in the Appendix A has the incident histories of 40,000 and 1.66 MeV electrons follows down to 0.05 MeV through the 0.6731 cm thick anode assembly. This run involved about 880,000 steps for the primaries, and the sampling of approximately 29,000 knock–ons and about 37,000 secondary histories. The run time required on the IBM mainframe and on the micro VAX 3200 workstation is summarized in the following Table III. The

computer run time depends largely on the secondary electron cutoff energy. Changing this cutoff to half would result in a run time smaller by about a factor of 10.

TABLE XIV : COMPUTATION TIME
(for the input file in Appendix A)

Major parameters	IBM main frame	micro VAX
40000 histories Electron energy (1.66 MeV to 0.05 MeV) 3 materials (Ta, Al, TLD)	56 minutes	45 minutes

APPENDIX F. MEASURED EXPOSURE VARIATION

Marx Charge 75 kV Series

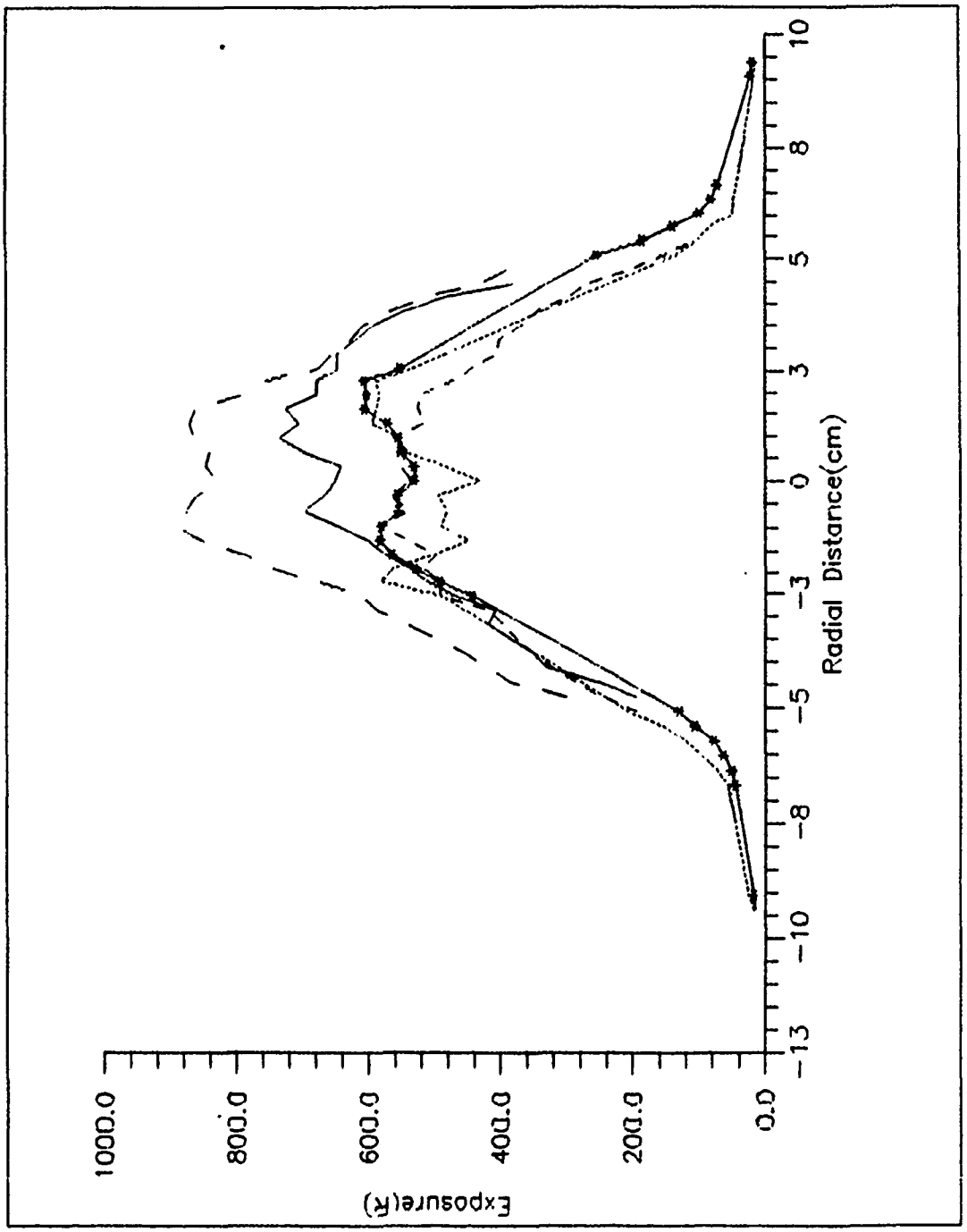

Marx Charge 100 kV Series

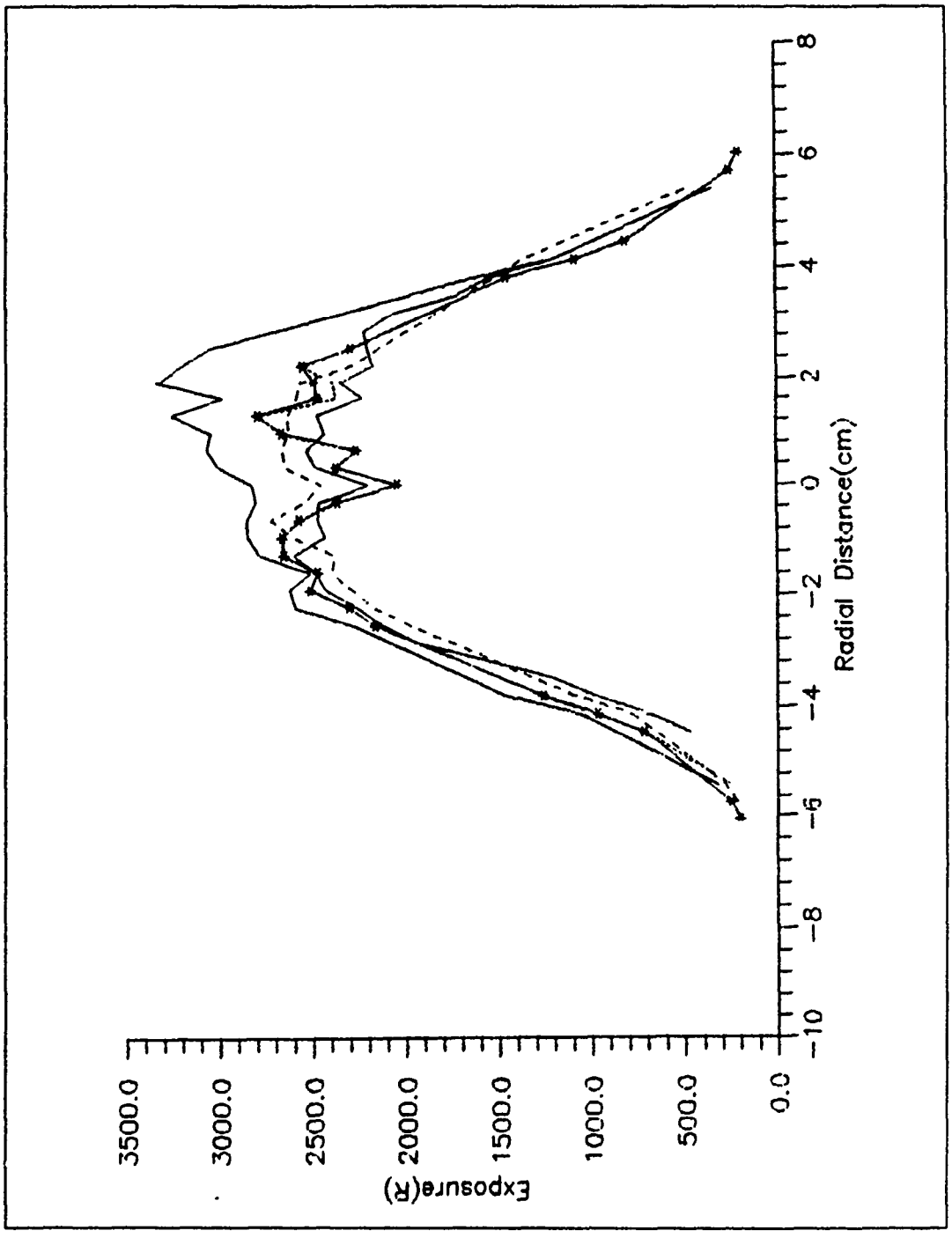

LIST OF REFERENCES

1. Pietruszka, R. B., *Operation and Characteristics of the Flash X–Ray Generator at the Naval Postgraduate School*, Master's Thesis, Naval Postgraduate School, Monterey, California, June 1989.

2. Miller, R. B., *An Introduction to the Physics of Intense Charged Particle Beams*, Plenum Press, 1982.

3. Physics International Company, *Model 112B Pulserad Plused X–Ray Generator Operations and Maintenance Manual*, February 1987.

4. Miller S., *ITS: The Integrated Tiger Series of Coupled Electron/Photon* Monte Carlo Transport Codes, Lawrence Livermore National Laboratory Report DDV–88–0031, December 1988.

5. Attix, F. H., *Introduction to Radiological Physics and Radiation dosemetry.* John Wiley and Sons, Inc., 1986.

6. Jenkins, T. M., Nelson, W. R. and Rindi, A., *Ed. Monte Carlo Transport of Electrons and Photons*, Plenum, 1988.

7. U. S. Army Laboratory Command Report HDL–TR–2107, *The Theory and Practice of Radiation Dosimetry in the Radiation Hardness Testing of Electronic Devices and Systems*, by K. G. Kerris, April 1987.

8. Berger, M. J., *Monte–Carlo Calculations of the Penetration and Diffusion of Fast Charged Particles*, in *Methods in Computational physics, Vol. 1*, edited by B. Adler, S. Fernbach and M. Rotenberg, Academic Press, 1963.

9. Stanford, T. W. L., and others, "Experimental Ckeck of Bremsstrahlung Dosimetry predictions for 0.75 MeV Electrons", *IEEE Trans. Nucl. Sci.*, Vol. NS–32, No. 6, December 1985.

10. Nation, J. A., "High Power Electron and Ion Beam Generation", *Particle Accelerators*, Vol. 10, pp. 1–29, 1979.

11. U. S. Department of Commerce, National Bureau of Standatds, *Report of the International Commission on Radiological Units and Measurement (ICRU)*, pp. 1–7, Government Printiong Office, Washington, DC, April 1957.

12. American Society for Testir . . . terials Standard E666–78, *Standard Practice for Calculating Ab . . . se from Gamma or X radiation*, 1988 Annul Book of ASTM Sta. . . ., Vol. 12.02, pp. 243–248, American Society for Testing and Materials, 1988.

13. Stanford, T. W. L. and Hablieb, J. A., "Radiation Output and Dose Predictions for Flash X–ray Sources",*IEEE Trans. Nucl. Sci.*, Vol. NS–31, No. 6, December 1984.

INITIAL DISTRIBUTION LIST

		No. Copies
1.	Defense Technical Information Center Cameron Station Alexandria, Virginia 22304–6145	2
2.	Library, Code 0142 Naval Postgraduate School Monterey, California 93943–5002	2
3.	Department Chairman, Code 61 Department of Physics Naval Postgraduate School Monterey, California 93943–5004	1
4.	Prof. Xavier. K .Maruyama, Code 61Mx Department of Physics Naval Postgraduate School Monterey, California 93943–5004	3
5.	Prof. John R. Neighbours, Code 61Nb Department of Physics Naval Postgraduate School Monterey, California 93943–5004	1
6.	Kim, Jong Ryul 500 Kwang–Ju Si, Book–Gu, Du–Am Dong, 874–14 Seoul, Korea	5
7.	Physics Library, Code 61 Department of physics Naval Postgraduate School Monterey, California 93943–5100	1
8.	Capt. Song, Tae Ik SMC 2686 Naval Postgraduate School Monterey, California 93943–5000	1
9.	Capt. Park, Jung Hyun SMC 1818 Naval Postgraduate School Monterey, California 93943–5000	1

10. Capt. Yoo, Jong Soo
SMC 2039
Naval Postgraduate School
Montery, California 93943–5000 — 1

11. Library
130–02
Korea Military Academy
Gong–Reung Dong, 556–21
Seoul, Korea — 1

12. Mr. Donald Snyder, code 61
Accelerator Laboratory
Department of Physics
Naval Postgraduate School
Monterey, California 93943–5100 — 1